

Air layers under water on the fern *Salvinia*
—
Stability and biomimetic applications

Dissertation

zur

Erlangung des Doktorgrades (Dr. rer. nat)

der

Mathematisch-Naturwissenschaftlichen Fakultät

der

Rheinischen Friedrich-Wilhelms-Universität Bonn

vorgelegt von

Matthias Mayser

aus

Neuss

Bonn, 2013

Angefertigt mit Genehmigung der Mathematisch-Naturwissenschaftlichen Fakultät der Rheinischen Friedrich-Wilhelms-Universität Bonn.

1. Gutachter: Prof. Dr. Wilhelm Barthlott
2. Gutachter: Prof. Dr. Kerstin Koch

Tag der Promotion: 28.05.2013

Erscheinungsjahr: 2014

Acknowledgments

This thesis was carried out as part of the collaborative research project 'Unter Wasser Luft haltende Schiffsbeschichtungen für die Reibungsreduktion an Schiffen' (grant 01RB0803A), funded by the Federal Ministry for Education and Research (BMBF) in the BIONA program.

I would like to thank my supervisor Prof. Wilhelm Barthlott for his support and inspiration throughout the thesis. His extensive knowledge of botany and biomimetics as well as his experience in presentations and collaborations were extremely helpful and enlightening.

Furthermore I would like to thank Prof. Kerstin Koch for co-supervising my work. I am very grateful for the encouraging discussions and the different perspectives of things she gave me on several occasions.

During my years in this project Dr. Holger Bohn, Dr. Petra Ditsch-Kuru and Dr. Ingo Scholz supervised me successively in my scientific approaches. Each of them deserve my sincere gratitude for their support while setting up, performing and discussing my experiments as well as for establishing a productive and pleasant working environment and encouraging me to pursue my ideas.

I would also like to thank Dipl.-Biol. Adrian Klein for the great collaboration on the replication technique and the countless activities we enjoy over the years.

I want to express my appreciation for the collaborations with the working groups of Prof. Alfred Leder of the chair of fluid mechanics (LSM, University Rostock) and Prof. Thomas Schimmel at the Karlsruhe Institut of Technology. I especially thank Dr. Stefan Walheim for the motivating discussions and ideas, Dipl.-Phys. Daniel Gandyra for generating the biomimetic *Salvinia*-effect surfaces and Dipl.-Phys. Matthias Mail for providing the biomimetic egg beater hair structures and keeping up the spirits and communication.

Hans-Jürgen Ensikat helped me substantially in the setup of the temperature control in my experiment and by sharing his extensive knowledge of SEM techniques.

I thank my former and present colleagues at the Nees-Institute, especially Anna Schulte how lived through the ups and downs of a PhD thesis with me. I would like to mention the diploma students Erik Schneider, Frederik Maurer-Wildermann, Dominic Mohr and Meike Reker, whose work helped completing the picture of air retention. Also substantial for a functional daily business were the secretary staff Elisabeth Gebhardt, Gabriele Hohmann, Rosemarie Pretscher and the late technical assistant Wolfgang Roden.

Very special thanks to the Botanical Gardens of the University of Bonn for building up and cultivating the collection of *Salvinia* plants.

I thank the members of the DFG Graduate Program GRK1572 "Bionik - Interactions across Boundaries to the Environment" for the scientific and nonscientific exchange and the workshops. Special thanks go to Dipl.-Inform. David Kriesel, whose help on LaTeX

contributed substantially to the creation of this thesis and who contributed to several conversations with his non-biological point of view.

Especially I want to thank my parents, Hanno and Angelika Mayser, on whom I could rely at any time, who supported me in all my decisions and encouraged. I also thank my brother Dr. Andreas Mayser and his family for all the support and good times they gave me.

Contents

1	General Introduction	1
1.1	Wetting	1
1.2	Superhydrophobicity	2
1.3	Air retention	4
1.4	Applications for air layers	5
1.5	Biological model organisms	6
1.5.1	Animals	6
1.5.2	Plants	8
1.5.3	Salvinia	9
2	Aim of this study	13
3	Air volume measurement by buoyancy	15
3.1	Materials and methods	15
3.1.1	Buoyancy measurement	15
3.1.2	Surface parameters of the <i>Salvinia</i> leaves	18
3.2	Results and Discussion	18
3.3	Conclusion	21
4	Long term air retention in Salvinia	23
4.1	Materials and Methods	23
4.1.1	Temperature control	23
4.1.2	Aerenchyma of <i>S. oblongifolia</i>	24
4.1.3	Measurement setup	26
4.2	Results and discussion	26
4.2.1	Progress of air volume changes	26
4.2.2	Rate of air volume changes	27
4.2.3	Air layer persistence	28
4.3	Conclusion	29
5	Stability of air layers under pressure fluctuations	31
5.1	Materials and methods	31
5.1.1	Pressure cell	31
5.1.2	Measurement setup	32
5.2	Results	33
5.2.1	<i>S. minima</i>	33
5.2.2	<i>S. molesta</i>	34
5.2.3	<i>S. oblongifolia</i>	34
5.2.4	<i>S. cucullata</i>	36
5.3	Discussion	37
5.3.1	Comparison of the pressure resistance	37
5.3.2	Regeneration of the air layer after depressurization	38

5.4	Conclusion	39
6	Technical surfaces for air retention	41
6.1	Flock surfaces	41
6.1.1	Materials and methods	41
6.1.2	Results and discussion	43
6.2	Artificial Salvinia-effect surface	44
6.2.1	Materials and methods	45
6.2.2	Results and discussion	45
6.3	Replication	46
6.3.1	Materials and methods	47
6.3.2	Results and discussion	48
6.4	Conclusion	50
7	Design of an optimized technical surface	51
	Summary	55
	Zusammenfassung	57
	List of Figures	59
	List of Tables	61
	Bibliography	63
	Publications	71

1 General Introduction

Every interaction of biological organisms with the surrounding are influenced essentially by their surface [Martin and Juniper 1970]. Over millions of year of evolution these surfaces got optimized to either improve this interaction or to protect the organism from harmful environmental conditions. Analyzing the natural surfaces and understanding their functionality does not just improve our knowledge of the biological processes but also reveals interesting opportunities to transfer and apply such functionalities in technical applications [Barthlott and Koch 2011]. One interesting surface property that could be used in a biomimetic transfer into technology is the capability of several plants and animals to maintain air layers under water for extended periods of time [Balmert et al. 2011; Solga et al. 2007; Heckman 1983]. These air layers could be used for drag reduction on ships [Fukuda et al. 2000], in pipes/pipelines [Fukuda et al. 2000] or in microchanelns and microfluidics [Kim and Kim 2002].

1.1 Wetting

Essential for the retention of an air layer under water is the wetting behavior of these surfaces. Wetting describes the state of contact between a surface and a fluid [De Gennes et al. 2004]. A drop of a certain liquid contacts a given surface always in the same way. This drop behavior can be described by the contact angle (Θ) that is being established between the liquid-solid and liquid-air contact lines at the point of three phase contact (Fig. 1.1).

This contact angle (CA) can be calculated as a function of the surface tensions of solid/gas (γ_{SG}), solid/liquid (γ_{SL}) and liquid/gas (γ_{LG}) according to Young's equation [Young 1805]:

$$\gamma_{SG} = \gamma_{SL} + \gamma_{LG} \cdot \cos\Theta \quad (1.1)$$

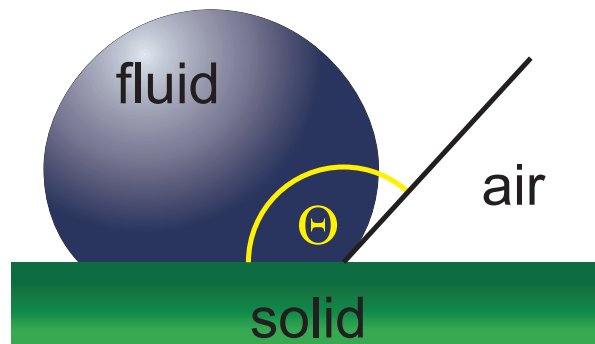


Figure 1.1: The contact angle established between liquid and solid

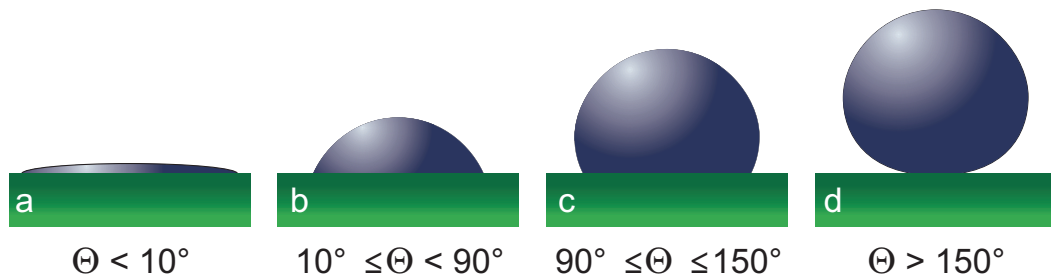


Figure 1.2: Scheme of drops on surfaces with different wetting behaviour, a) superhydrophilic, b) hydrophilic, c) hydrophobic, d) superhydrophobic

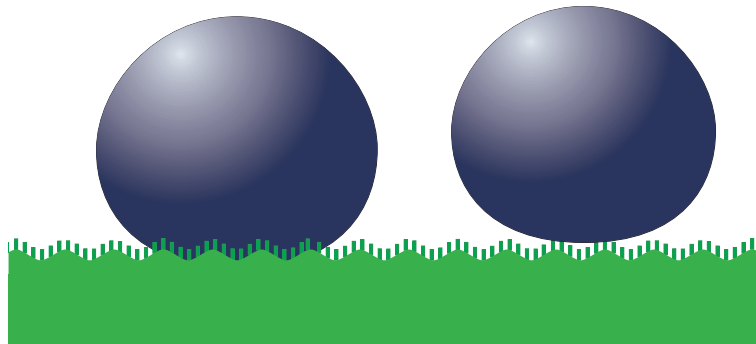


Figure 1.3: Scheme of a drop on a rough surface in Wenzel state (left) and Cassie-Baxter-state (right)

Increasing contact angles imply the decreasing ability of water to wet the surface and thereby result in a more spherical shape of the drop sitting on surface. A static CA below 90° indicates an attraction to water (hydrophilicity) while contact angles above 90° are characteristic for hydrophobic materials (Fig. 1.2), which do not bond well with water [De Gennes 1985]. The maximal CA of water possible on a flat, smooth surface is 120° [Nishino et al. 1999].

However, strictly speaking Young's equation is only applicable on flat, homogeneous surfaces. If the surface displays roughness or is comprised of different materials on a small scale, the solid's surface tension differs from the one calculated by Young's equation. This also applies to most biological surfaces as they are rarely flat and homogeneous. Roughness on the surface increases both hydrophilicity and hydrophobicity [Wenzel 1936]. The state of extreme hydrophobicity is called superhydrophobicity, while extremely hydrophilic surfaces are called superhydrophilic. There are several definitions of superhydrophobicity and superhydrophilicity in existence but often superhydrophobicity is assumed at CAs above 150° and superhydrophilicity at CAs below 10° (e.g. by Koch et al. [2008a]; Jung and Bhushan [2006]; Bhushan et al. [2007]; Roach et al. [2008]) (Fig. 1.2).

1.2 Superhydrophobicity

For superhydrophobicity to occur a hydrophobic chemistry of the material is mandatory. Additionally micro structures have to induce a roughness to further increase the contact angle. With these types of superhydrophobic surfaces different states of wetting are

possible. In the Wenzel-state the whole surface is wetted by water (Fig. 1.3 left) Wenzel [1936]. In this state the contact angle Θ_W can be calculated from the contact angle of the material and the relation of real surface area A to projected surface area A_P :

$$\Theta_W = \frac{A}{A_P} \cdot \Theta \quad (1.2)$$

As the distance of the surface structures gets smaller and the ratio between real and apparent contact area increases, it becomes energetically favorable for the water drop not to cover the whole surface but to sit on the tips of the micro structures of the roughness leaving air pockets below the water (Fig. 1.3 right). The contact area of the drop is accordingly comprised of the solid of the surface as well as the air in between [Cassie and Baxter 1944]. In this Cassie-Baxter-state the contact angle Θ_{CB} can be calculated to

$$\Theta_{CB} = f_{LS} \cdot \Theta - f_{LG} \quad (1.3)$$

with f_{LS} being the fraction of liquid-solid-contact below the drop and f_{LG} the fraction of liquid-air-contact. It is obvious from the equation that a reduction of the solid-liquid contact fraction leads to a higher hydrophobicity and a higher contact angle. So minimizing this fraction is a general principal to generate non-wettable surfaces [Wagner et al. 2003].

Adding more levels of structuring increases the contact area in the Wenzel-states and decreases the water solid contact in the Cassie-Baxter-state. Therefore a hierarchical structuring of a surface increases its superhydrophobicity [Koch and Barthlott 2009].

But the Cassie-Baxter-state is not a stable state. The water can penetrate in between the structures and perform a transition to the Wenzel-state, which was thought to be irreversible [Qu er e et al. 2003]. This transition can be induced by pressure, which would compress the air trapped between the structures with the surrounding water filling the gaps [Yu et al. 2006]. Another scenario for the transition could be observed during evaporation, where small droplets would penetrate the air pockets as they were getting smaller during evaporation [McHale et al. 2005]. More recent approaches demonstrated possibilities to perform a Wenzel-Cassie transition by electrolysis of water [Lee and Kim 2011], heating [Liu et al. 2011], pressure [Forsberg et al. 2011; Verho et al. 2012]. However in the last case the water only penetrates the coarsest level of structuring while Cassie-state is preserved on the nano scale. So it does not represent a real Wenzel-state.

As the contact angle does not reveal the state of wetting (Cassie-Baxter or Wenzel) other factors are commonly used to better characterize superhydrophobicity [ oner and McCarthy 2000]. The tilt angle describes the inclination of the surface at which a drop lying on the surface starts to roll off [Furmidge 1962]. High tilt angles are characteristic for a drop in the Wenzel-state as the water is in contact with a relatively large surface area, so the adhesion to the surface is increased [Chen et al. 1999]. The opposite can be observed for the Cassie-Baxter-state, in which the contact surface area is small compared to the drop and it rolls off at very low tilt angles. A tilt angle below 10° is therefore often used as an additional criteria for superhydrophobicity [Koch et al. 2009].

Those superhydrophobic surfaces with high contact angles and low tilt angles often display a self cleaning ability. Firstly described by Barthlott and Neinhuis [1997] on the Lotus plant (*Nelumbo nucifera*) the low fraction of contact area responsible for the superhydrophobicity also leads to a reduced contact between contamination particles and



Figure 1.4: An air layer under water; visible by the silvery reflection on a submerged water fern *S. oblongifolia*, Foto: P. Schoppa/Fraunhofer Institute UMSICHT/BMBF

the surface. Even for hydrophobic particles the adhesion to the surface is lower than to a drop rolling across it. So the water drop picks up the contamination and washes it off the surface. Following this discovery the importance of and work on superhydrophobicity has ever been increasing [Gao and McCarthy 2007, 2009]. Several production methods for artificial superhydrophobic surfaces have been developed [Yan et al. 2011], often involving nanotechnology [Bhushan 2004].

1.3 Air retention

The retention of air layers under water (Fig. 1.4) obviously requires a Cassie-Baxter-state, which results in hydrophobic surface chemistry [Callies and Quéré 2005] and hierarchical structured surface [Lakes 1993; Koch et al. 2009] being prerequisites for air retention.

Solga et al. [2007] identified five factors relevant for air retention. Apart from the hydrophobic surface chemistry they state that hairy micro structures combined with an overlaying nano structure along with cavities and an elasticity of the structures is beneficial for long term air retention. While the cavities increase the ratio of real to apparent surface area and thereby the hydrophobicity, elasticity is important in changing surrounding conditions like pressure fluctuations. Elastic hairs can follow the resulting movements of the air water interface and prevent a progression of wetting towards the base of the structures [Otten and Herminghaus 2004].

A further important factor is the density of the structures [Crisp 1950]. High densities have been correlated with long air layer persistence [Balmert et al. 2011] as the support of the air water interface is increased by many contact points and a high contact line length. It has also been shown that an equal distribution of the hairs increases the stability of air

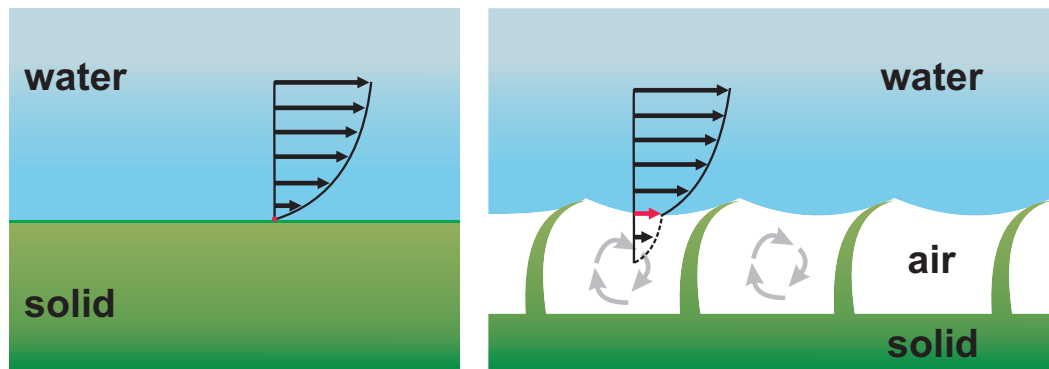


Figure 1.5: Scheme of principle of drag reduction by air layers; on a non-air-retaining surface the water sticks to the surface at the boundary layer (left), with an air layer the air water interface can flow with the water (right)

layers because higher local distances between adjacent hairs could provide a weak point of the superhydrophobicity [Thorpe and Crisp 1947b; Flynn and Bush 2008].

Along with the increased research activity concerning under water air retaining surfaces multiple techniques for the generation of technical air retaining surfaces have been presented. An overview of several of these techniques can be found at Yan et al. [2011].

1.4 Applications for air layers

There are various technical applications for air layer under water.

Probably the most appealing and most discussed application is drag reduction [Fukuda et al. 2000; Balasubramanian et al. 2004; Choi and Kim 2006; Fukagata et al. 2006; McHale et al. 2010]. An under water air retaining surface would decrease the solid water contact area by up to 95% [Cheng et al. 2006]. While there is a non slip condition between the flowing water and the underlying solid, the air water interface in between the structures is capable of flowing with the water (Fig. 1.5). Because of the lower viscosity of the air compared to the water the movement in the air causes less drag and thereby reduces the overall drag [McHale et al. 2011]. According to previous calculations and experiments the drag could be reduced by up to 55% [Choi and Kim 2006; Fukagata et al. 2006; McHale et al. 2010].

This drag reduction could be used for example on ship hulls. In ship transports up to 80% of the propulsion energy is consumed by drag [Fukuda et al. 2000]. So an improvement in this aspect would have a high economic and ecological impact [Eyring et al. 2010; Corbett and Koehler 2003]. Assuming 70% drag on ships and 10% drag reduction by an air retaining ship hull, the application of the coating on world wide shipping would result in a decrease of the worldwide total oil consumption by 1% (according to International Energy Agency [2009]).

Previous attempts of reducing drag by air bubbles being introduced into the water around a ship ('micro bubbles technique') were thought of by Paffett [1972] and later realized by Kodama et al. [2003]. However, the efficiency of the method was reduced by the energy consumption of the pumps which would pump the air into the water Kodama et al. [2003].

As an air retaining surface would hold an air layer passively this drawback would not apply here.

Furthermore there have been speculations of air layers acting as an anti-fouling agent [Marmur 2006a]. This would decrease the pollution of the sea by toxic substances currently used to prevent the fouling of ship hulls by alga, Balanidae (a family of barnacles of the order *Sessilia*) and mussels and further increase the ecologic value of such an air retaining coating.

The drag reducing effect could also be used in microfluidics/micro channels [Kim and Kim 2002] or pipelines. Other potential applications for under water air retaining surfaces include swimsuits, thermal or chemical insulation.

A problem so far has been the stability of the air retaining surfaces in testing. The air layers lasted only a few minutes to hours in the flow [Balasubramanian et al. 2004; Marmur 2006b]. So research for more stable air layers is necessary for the technical application.

1.5 Biological model organisms

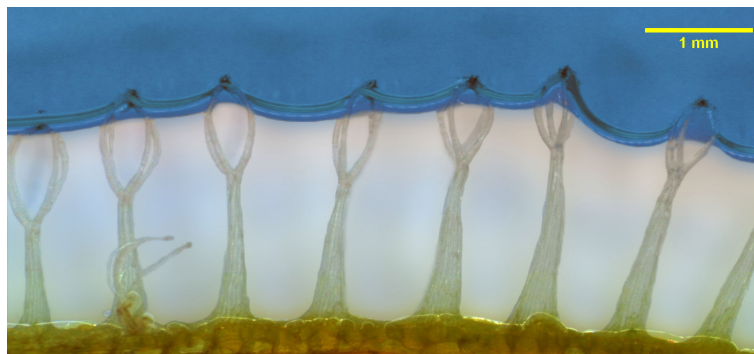


Figure 1.6: Side view of an air layer on *Salvinia molesta*, Foto: E. Schneider & M. Mayser

In nature there are several aquatic or semi-aquatic plant and animal species, which are capable of maintaining air layers over short or extended periods of time (Fig. 1.6).

1.5.1 Animals

Functions

Air retaining surfaces may serve several purposes for the animals. Insects not living in the water usually use the superhydrophobic properties of their air retaining surfaces to prevent drowning in case of accidental submergence [Heckman 1983] or to enable them to walk on the surface [Bush and Hu 2006]. This is usually achieved by a comparatively sparse cover of coarse hair, which do not adhere to each other by capillary forces and are capable to withstand a certain degree of pressure [Perez Goodwyn 2009].

For temporary or permanently submerged species the air layer may have different advantages. The most commonly found function of gas films is respiration. This can either be

realized in form of a compressible gas lung [Parsons 1971] or as a real plastron (also called physical gill) [Thorpe and D.J. 1947]. The later is a thin gas film of constant volume, which does not have to be refreshed by surfacing and covers parts of the animal body (especially the spiracle called openings of the respiratory system) [Thorpe and D.J. 1947; Thorpe and Crisp 1947a,b]. A plastron is maintained by a dense cover of small hairs (microtrichia), which are bent parallel to the air water interface at the tip to counter the hydrostatic pressure and keep the volume constant Perez Goodwyn [2009]. As oxygen from the air layer is consumed by the animal the partial pressure of oxygen in the gas phase falls while the partial pressure of carbon dioxide rises. This causes diffusion of CO_2 into the water and of O_2 into the plastron; thereby maintaining a constant reservoir over time [Messner and Adis 1996]. As plastrons have an infinite persistence they might have been an ideal model system for a ship coating. However, the amount of water solid interface of the whole surface is quite high which contradicts the principle of drag reduction by a low water solid fraction [McHale et al. 2010].

Compressible gas lungs are gas layers with decreasing volume over time. They are comprised of hairs with a different architecture, which are not stable and dense enough to antagonize against the water pressure leading to a diffusion of nitrogen into the water [Eriksen et al. 1995]. Although the compressible gas lung has the diffusive functionality as a plastron [Ege 1915], because oxygen diffuses trice as fast as nitrogen [Wigglesworth 1984], the air volume decrease continuously [Parsons 1971]. So the animals have to regenerate their reservoir regularly by surfacing [Hutchinson 1981].

A further use of air layers is thermal insulation. Calder [1969] proved a reduction of heat loss by 50% caused by the air layer of the water shrew (*Sorex palustris*). It has also been shown that the balance system of *Aphelocheirus aestivalis* relies on an air layer because the related mechanosensors are not functional in the water [Larsén 1955]. Furthermore improved control of buoyancy [Vogel 2006] as well as improved locomotion on and under water Suter and Wildman [1999]; Suter et al. [2004] have been discussed. The air retaining elytra of the back swimmer *Notonecta glauca* (Fig. 1.7) enable the insect to take flight right out of the water and might even reduce the drag.

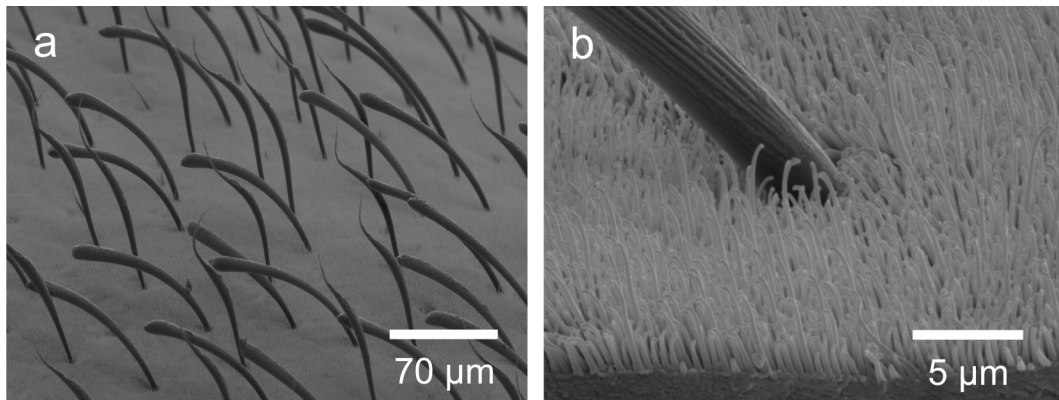


Figure 1.7: The surface structures on the air retaining elytra of *N. glauca*, a) overview (setae & microtrichia), b) detail (microtrichia)

Appearance

Amongst animals air retention is found in secondary aquatic or semi-aquatic species. It has been developed several times in different taxa and represents a convergent evolution [Heckman 1983]. Air retention is most common in the phylum Arthropoda but also known for a few mammals. In the family of shrews (Soricidae) there are several genera capable of maintaining an air layer under water in their dense fur [Calder 1969; Beneski and Stinson 1987; Köhler 1991].

Heckman [1983] gives broad overview of air retention in arthropods.

In the class of arachnids (Arachnida) several species display air retaining surfaces either for walking on the water surface (e.g. the fishing spider *Dolomedes triton* [Suter et al. 2003]) or respiration under water (e.g. *Phrynus marginemaculatus* [Hebets and Chapman 2000], water spider *Argyroneta aquatica* [Heckman 1983]). Their surfaces are mostly comprised of a dense cover of bristles, each lined with rows of spines [Heckman 1983].

The most species with under water air retention can be found among insects [Heckman 1983], especially in bugs and beetles. Balmert et al. [2011] compared the air layer persistence of several non-plastron surfaces of insects. In this survey the elytra of the back swimmer *Notonecta glauca* displayed the longest air retention with more than 120 days (longer than 130 days according to Ditsche-Kuru et al. [2011b]). The functional structures on these elytra (Fig. 1.7) are a dense cover ($6 \times 10^6/mm^2$) of short microtrichia combined with two different types of sparser set setae ($250/mm^2$ [Ditsche-Kuru et al. 2011b]), creating a double structuring.

1.5.2 Plants

A lot of plants are known to be superhydrophobic (most famously the lotus *Nelumbo nucifera*). Most of these are found either close to or in the water or in areas prone to floods [Neinhuis and Barthlott 1997]. Their superhydrophobicity enables them to secondarily populate aquatic or semiaquatic habitats and survive temporary submergence.

Functions

An air layer provides two ecological advantages for secondary aquatic plants:

It adds additional buoyancy if the plant gets submerged despite the buoyancy of the internal air reservoir in the aerenchyma [Kaul 1976]. This increases the ability to resurface and renders floating plants more capable of spreading out instead of covering each other.

Furthermore an air layer enables the plants to maintain a higher level of photosynthetic activity when submerged [Raven 2008]. A water film on a plant adapted to air respiration reduces the exchange of gases, leading to inefficient photosynthesis and stress for the plant [Colmer and Pedersen 2008]. An air film serves as a plastron (as described for insects) and promotes the exchange of oxygen and carbon dioxide.

Appearance

The surfaces of most superhydrophobic plants are comprised of papillae covered by coating of 2D and 3D wax [Koch et al. 2009; Koch and Ensikat 2008]. However, the air layers of such papillose surfaces are relatively thin and not very stable [Balasubramanian et al. 2004]. So for purpose of drag reducing coatings plants with larger air volumes and longer air layer persistence are better suited, which is known for hairy plant surfaces [Barthlott et al. 2010].

Such hairy, air retaining surfaces can be found on the tropical and subtropical, floating water cabbage (*Pistia stratiotes*) in the family Araceae. Several species can also be found in the order Salviniiales including *Marsilea hirsuta* and all species of the genus *Salvinia*.

1.5.3 *Salvinia*

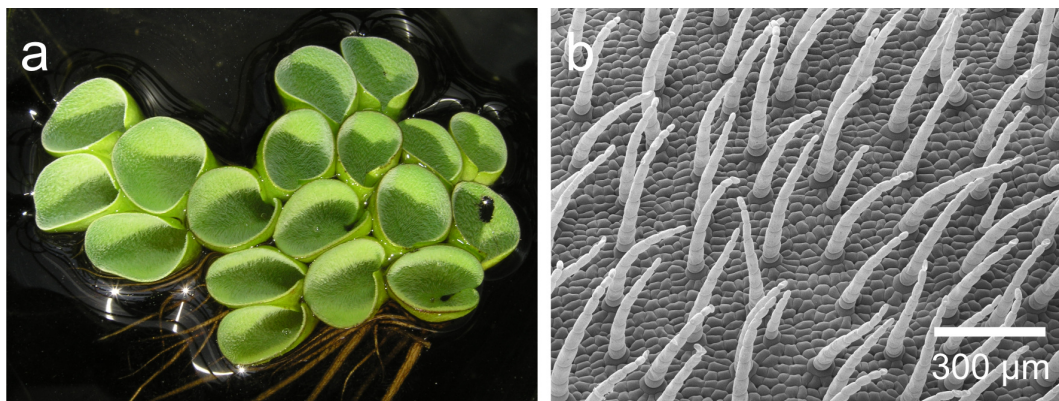


Figure 1.8: *Salvinia cucullata*, a) habitus, b) SEM picture of the trichome structures

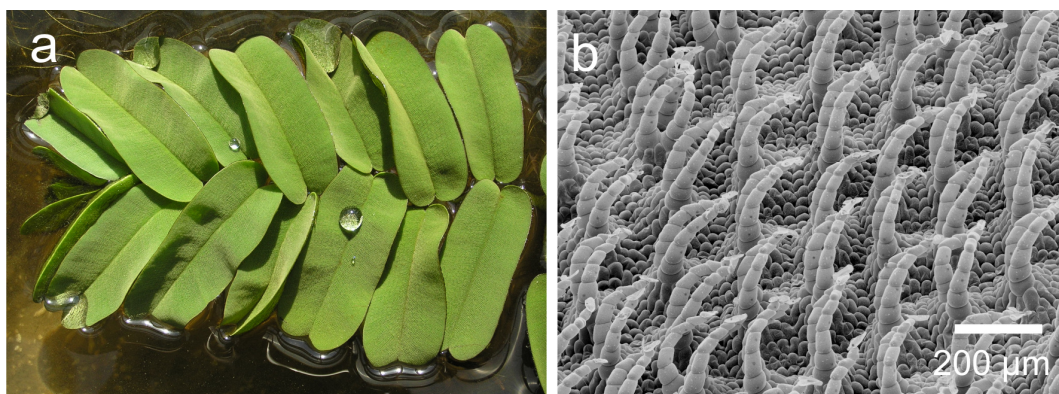


Figure 1.9: *Salvinia oblongifolia*, a) habitus, b) SEM picture of the trichome structures

Salvinia are tropical floating ferns of the class Polypodiopsida, most of which are found in South America. They are very fast spreading, mat forming plants [Jacono et al. 2001] and pest plants in several tropical and subtropical waters [Julien et al. 2002], where they clog water ways and suppress native plants and animals.

Although the taxonomic status in this genus is not well supported, there are currently 10 species recognized according to [Schneller 1990], which are differing in leaf and trichome

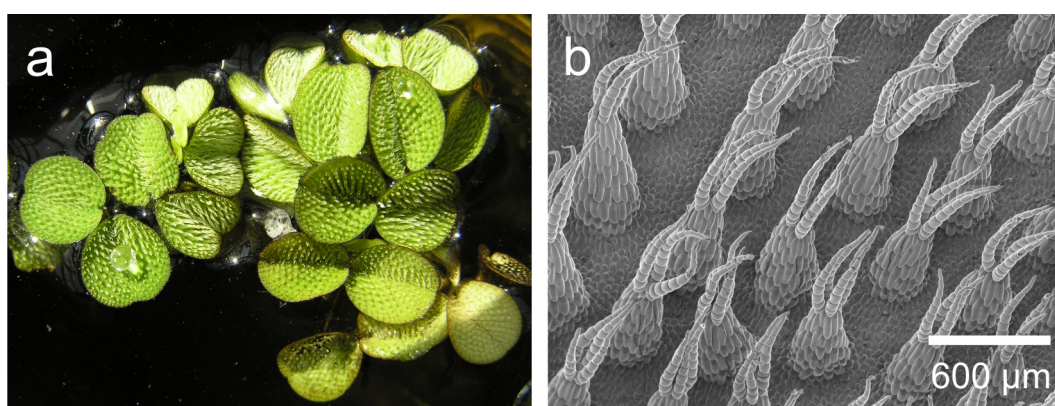


Figure 1.10: *Salvinia minima*, a) habitus, b) SEM picture of the trichome structures

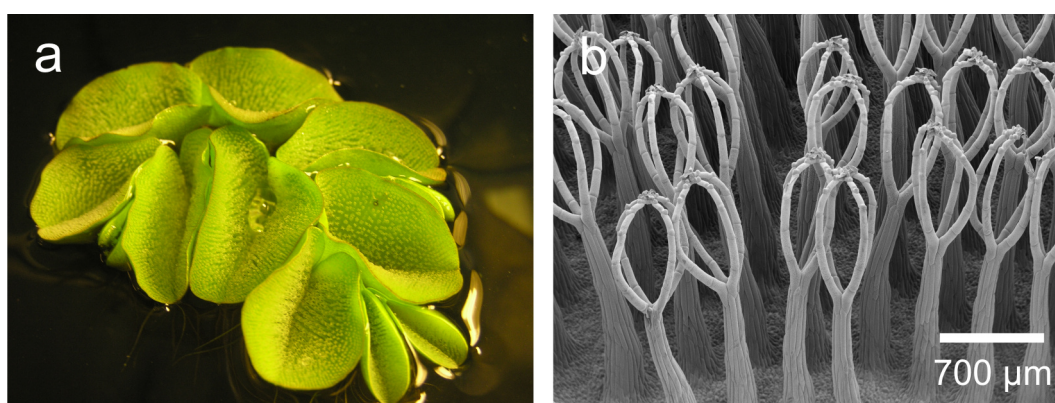


Figure 1.11: *Salvinia molesta*, a) habitus, b) SEM picture of the trichome structures

morphology [De la Sota 1977]. Because each species can develop a variety of different leaf forms and trichome structures several more species have been described by mistake [Herzog 1934]. *S. natans* is the only species native to Germany.

Salvinia grows with a creeping stem and leaves in whorls of three. One of these is finely dissected, root like and submerged while the other two are floating on the surface with a superhydrophobic upper surface, which is hierarchically structured by trichomes, convex cells and wax crystals. The wax crystals are thin rodlets perpendicular to the surface [Barthlott et al. 1994; Barthlott 1990; Barthlott and Wollenweber 1981].

There are four different trichome shapes described [Barthlott et al. 2009].

The Cucullata type displays simple, slightly curved hairs, consisting of 6 to 8 cells in a row (Fig. 1.8) and is present in *S. cucullata* and *S. hastata*. The Oblongifolia type incorporates trichomes which consist of two hairs, which grow out of a shallow, dome shaped emergence and are joined at their topmost cells (Fig. 1.9). Four hairs growing on top of a large emergence which are not joined at their tips are called Natans type (Fig. 1.10) and are found on *S. natans* and *S. minima*. The so called 'egg beater hairs' (found on *S. molesta*, *S. biloba* and *S. auriculata*) consist of a tall emergence topped with four hairs which are joined at their tips (Fig. 1.11).

A special feature has recently been described of the trichomes of *S. molesta*. The four topmost cells of the egg beater basket are dead and have lost their hydrophobizing waxes. This leads to these cells forming a hydrophilic tip on the otherwise superhydrophobic

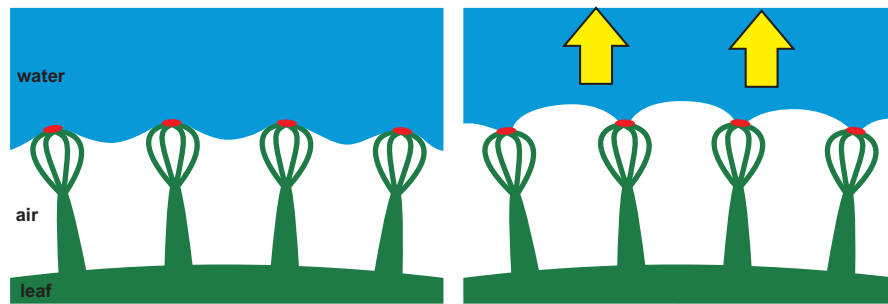


Figure 1.12: Scheme of the Salvinia[®]-effect; normal pressure (left), at low pressure (yellow) the hydrophilic tips of the hairs (red) pin the air water interface to the hairs and prevent the extraction of air bubbles (right), modified after [Barthlott et al. 2010]

hair. Submerged the hydrophilic tip pins the air water interface to the hair and prevents the formation of air bubbles (Fig. 1.12). Accordingly this so called "Salvinia[®]-effect" stabilizes air layers in turbulent conditions and low pressure scenarios [Barthlott et al. 2010].

2 Aim of this study

In previous studies in the working group of Prof. Barthlott at the Nees Institute for Biodiversity of Plants starting in 2002 the potential of superhydrophobic, air retaining, biological organisms have been examined, funded by the Deutsche Bundesstiftung Umwelt DBU and the Federal Ministry for Education and Research BMBF (grant PTJ-BIO/311965/A).

A first screening of potential model organisms identified a number of animals and plants (including *Neomys*, *Ancylometes*, *Gerris*, *Notonecta*, *Pistia*, *Salvinia*,...), which are capable of maintaining air layers. In a following project the previously identified model organisms were further investigated, their air layer persistence tested and the morphology of the air retaining hair characterized. The back swimmer *Notonecta* and water ferns of the genus *Salvinia* were identified as the ideal model organisms and first air retaining textile surfaces were produced.

This study analyzes four species with different hair types of the genus *Salvinia* selected in order to identify the surface structure parameters relevant for air retention and to investigate their influence on air layer stability under different conditions. Further more these findings are transferred into technical application to design a prototype surface. This study is divided in four sections with subsequent questions:

Air volume measurement by buoyancy (Chapter 3). This chapter focuses on the air volume of air layers. For this purpose a new measurement setup that is capable of monitoring the air volume on air retaining surfaces is established, tested and applied. Which air volumes are held by the different species? Which influence do the leaf edges and the hair shapes have on the air volume?

Long term air layer stability (Chapter 4). In this chapter the previously build measurement system is used to monitor air layers over time and detect the long term air layer stability. How long do the different *Salvinia* species retain an air layer? Which hair characteristics increase the air layer persistence?

Stability of air layers under pressure fluctuations (Chapter 5). This chapter investigates the stability of the air layer under pressure conditions like they would occur on ship hulls by hydrostatic or hydrodynamic pressure. Up to which pressures do the air layers of the different species exist? Which hair and leaf shapes are beneficial for air layer stability under pressure? Do the air layers reform to their original state after reducing the pressure?

Technical surfaces for air retention (Chapter 6). This chapter aims for the technical application of the air layers and tests findings of previous chapters on technical surfaces. Which effect do hair parameters have on air layer persistence? Do the hydrophilic pins of the *Salvinia*[®]-effect influence the air layer persistence under static conditions? How can sophisticated hair structures be produced in large scale?

In parallel diploma theses of Erik Schneider and Meike Reker these questions and methods were also applied on the back swimmer *Notonecta*.

3 Air volume measurement by buoyancy

Though the air layers held by *Salvinia* leaves have previously been studied qualitatively, the amount of air, held in this layers, has never been quantified. In this study a new method to measure the volume of air layers quantitatively and investigate the air volumes held by *Salvinia* leaves and artificial surfaces is presented.

3.1 Materials and methods

In order to test the method with a well defined, structured surface, silicon wavers with pillars of 60 μm height and a rectangular pattern with 60 μm diagonal pitch (Fig. 3.1a) were replicated with epoxy resin (Injection Resin EP, Reckli GmbH, Germany) as described by Koch et al. [2008a]. Replicas were hydrophobically coated with 25 μl of diluted (1:10) Tegotop 210 (Evonik Degussa GmbH, Germany) (Fig. 3.1b).

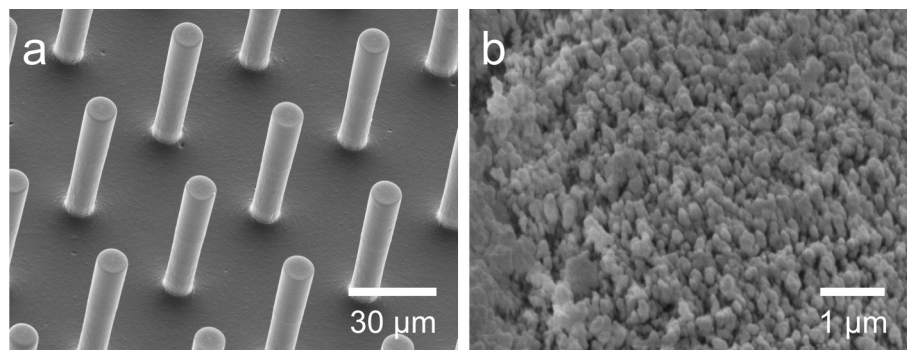


Figure 3.1: SEM images of a uncoated epoxy-resin replica of a) silicon wafer with pillars of 10 μm diameter and 60 diagonal pitch, b) hydrophobic coating of the replicas with Tegotop 210 in high resolution

Fresh leaves of four different *Salvinia* species incorporating all described trichome types [Barthlott et al. 2009] were measured. *S. cucullata* (BG BONN 18268) displays Cucullata type hairs (Fig. 3.2a), *S. oblongifolia* representing the Oblongifolia type (Fig. 3.2b), *S. minima* for the Natans type (Fig. 3.2c) and the so called 'egg beater hairs' on *S. molesta* (BG BONN 14459) (Fig. 3.2d). All plants were cultivated in the Botanical Gardens of the University of Bonn.

3.1.1 Buoyancy measurement

The air volume held by a surface was monitored by measuring the buoyancy the air generates. This has been accomplished by installing a silicon bending beam with two integrated strain gages (Sensor Element AE801, HJK, Germany) right above water level

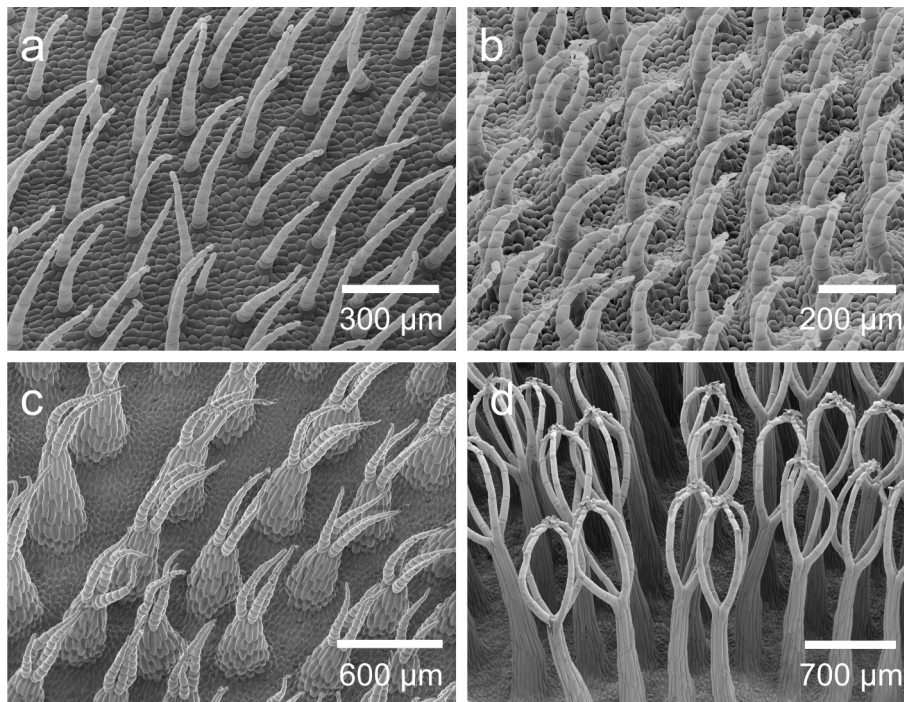


Figure 3.2: SEM images of upper leaf surface of four *Salvinia* species a) *Salvinia cucullata*, b) *S. oblongifolia*, c) *S. minima*, d) *S. molesta*

in an aquarium. A needle was then glued onto the beam with resin glue and bend to form a dent under water to which the samples could be attached (Fig. 3.3). The difference in strain gage resistance generated through the bending of the beam by buoyancy forces was measured by means of a Wheatstone half bridge (including a $1k\Omega$ resistor and the rotary potentiometer), an amplifier (G1T8, ME Meßsysteme GmbH, Germany) and a A/D converter (NI-USB6009, National Instruments, USA) (Fig. 3.4). The amplifier was reset to zero with the Wheatstone bridge adjusted to -10 V output signal to set the amplifier to 10 V output at neutral state. This allowed a measurement range of 20 V. The recorded voltages were then converted into forces through a calibration acquired with a set of 9 weights in the range from 1 to 700 mg. The calibration led to a factor of 45.25 mg/V for the setup and revealed a highly linear behavior across the whole measurement range (Fig. 3.5). The buoyancy force of air under water equals the weight difference to the displaced water; accordingly 45.25 mg/V equals 45.25 μl of submerged air per Volt assuming a water density of 1 mg/ μl . The maximum resolution of the measurement was 0.09 μl .

The volume retained by an air layer was measured on the wafer replicas as well as on leaves of four different species of the water fern *Salvinia*. In case of *S. cucullata* we took care not to have an air bubble trapped in the hood shaped leaf as this proved to not be very reproducible and detached air bubbles could stick to the measurement needle altering the measurement. First a sample with an air layer was attached to the needle and given 10 seconds to stabilize before the buoyancy was recorded (mean value over 10 seconds). Then the sample was detached from the needle, taken out of the water and covered with 70% ethanol for wetting the surface. After that it was washed for 20 seconds in water and then reattached to the needle for renewed buoyancy measurement.

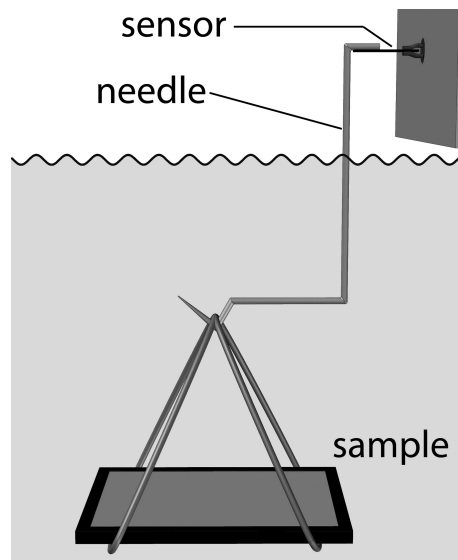


Figure 3.3: Schematic drawing of the measurement setup: A needle is glued to a silicon strain gage sensor and submerged under water; a wafer replica with air layer is hung onto the needle by nylon string.

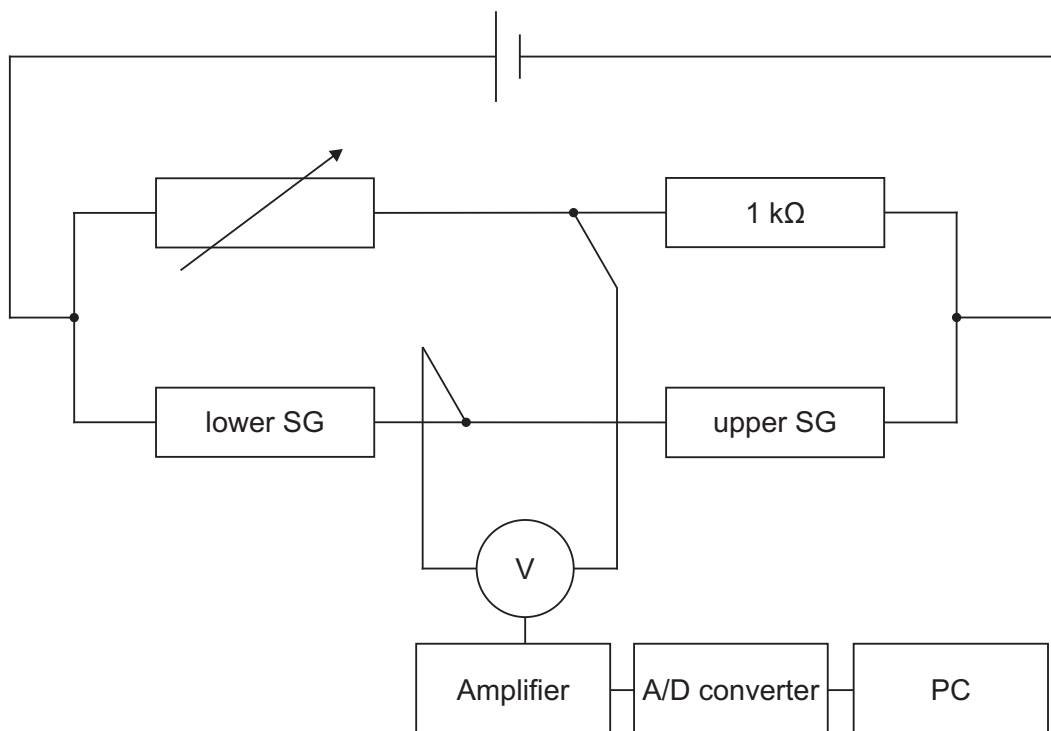


Figure 3.4: Circuit diagram of the measurement setup: The two strain gages (lower SG & upper SG) building a Wheatstone half bridge with the $1\text{ k}\Omega$ resistor and the rotary potentiometer. Buoyancy forces are measured as voltage changes by the voltmeter V

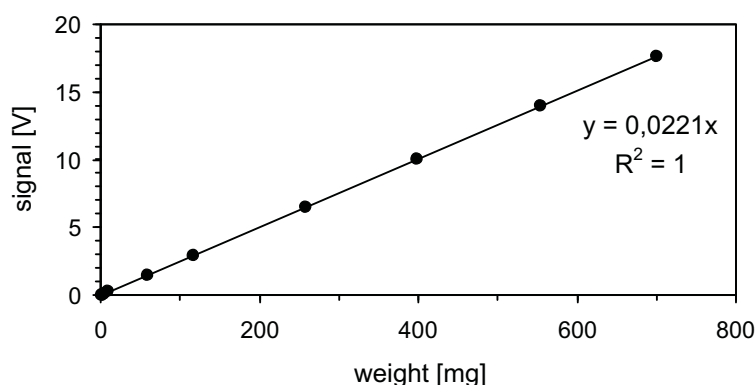


Figure 3.5: Calibration line of the measurement setup/force transducer using 9 weights in the range between 1 and 700 mg.

From the difference in buoyancy before and after removal of the air layer its volume was calculated.

3.1.2 Surface parameters of the *Salvinia* leaves

The leaf surface area was acquired after the volume measurement by scanning the flattened leaf with a flat bed scanner (Canon 4200F, Canon Inc., Japan) and measuring the leaf area on the image according to a calibration grid. A digital optical microscope (VHX-1000, Keyence, Japan) was used to measure the hair dimensions of the examined *Salvinia* species. Images of fresh leaves were taken from straight above and sideways in order to measure height, width and diameter of the trichomes as well as the hair density.

3.2 Results and Discussion

The measurement of the surface structure characteristics is summarized in Table 3.1.

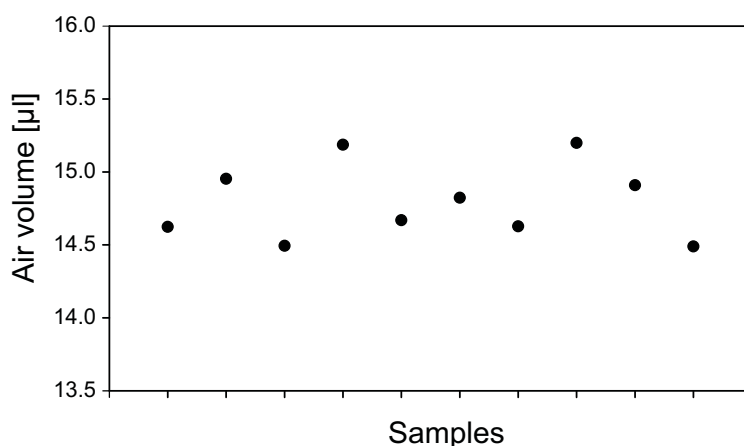


Figure 3.6: Air volume measured on replicas of structured wafers (● mean values averaged over 10s). Most values are slightly below the calculated theoretical air volume of $15.1 \mu\text{l}$.

Table 3.1: Structure characteristics of 4 selected *Salvinia* species (m \pm s.d., n=10)

		<i>S. oblongifolia</i>	<i>S. cucullata</i>	<i>S. minima</i>	<i>S. molesta</i>
hair density	1/mm ²	25.8 \pm 3.3	13.0 \pm 2.6	2.3 \pm 0.2	1.6 \pm 0.2
hair height	μ m	310 \pm 41	558 \pm 143	919 \pm 107	2.629 \pm 285
hair length	μ m	370 \pm 46	609 \pm 152	995 \pm 108	2.922 \pm 264
emergence length	μ m	177 \pm 30	<i>n.a.</i>	443 \pm 93	1.955 \pm 302
egg beater crown length	μ m	<i>n.a.</i>	<i>n.a.</i>	<i>n.a.</i>	967 \pm 51
trichome length	μ m	222 \pm 28	609 \pm 152	562 \pm 46	<i>n.a.</i>
emergence diameter (base)	μ m	269 \pm 8	<i>n.a.</i>	287 \pm 18	590 \pm 45
emergence diameter (tip)	μ m	168 \pm 13	<i>n.a.</i>	140 \pm 11	177 \pm 13
egg beater hair diameter	μ m	<i>n.a.</i>	<i>n.a.</i>	<i>n.a.</i>	613 \pm 73
trichome diameter (base)	μ m	68.5 \pm 6.8	40.5 \pm 6.3	71.2 \pm 6.9	71.0 \pm 6.7
trichome diameter (tip)	μ m	26.5 \pm 4.8	9.6 \pm 1.3	20.9 \pm 3.0	<i>n.a.</i>
leaf surface area	mm ²	1388 \pm 149	224 \pm 23	43.7 \pm 7.8	359 \pm 52

To evaluate the method the measured values were compared to the calculated theoretical air volumes of the micro structured replicas. The fraction of air per total surface area F_A on these replicas is

$$F_A = 1 - 2\pi(r/a)^2 = 0.956 \quad (3.1)$$

with r being the pillar radius and a the diagonal pitch of the pillars. The structured area displays a length l of 18.8 mm, a width w of 14 mm and 60 μ m pillar height h . Assuming a smooth air water interface the theoretical air volume V_A can be calculated to

$$V_A = l \cdot w \cdot h \cdot F_A = 15.1\text{mm}^3. \quad (3.2)$$

The air volume held by the micro structured replicas was measured to a mean value of $14.8 \pm 0.3\mu\text{l}$ (Fig. 3.6).

The measured mean air volume of the artificial micro structured surfaces represents the theoretical value nicely. It is approximately 2% below the theoretical air volume, which lies within the standard deviation. The slightly lower values might also be explained by the shape of the air water interface, which is not smooth but sagging in between the pillars, so that the real air volume should be slightly smaller than the value calculated above. Another reason could be defects in the hydrophobic coating, leading to small areas, where there might have happened a transition to the Wenzel wetting state thereby reducing the air volume of the sample.

The air volumes measured for four different *Salvinia* species have been normalized over the leaf surface area and plotted against the surface area (Fig. 3.7). The normalized air volumes show a close correlation to leaf size for each species. As the trichomes decrease in height towards the leaf edges, the air volume per leaf area also decreases towards the leaf edges. Idealizing a leaf as a circle, the edge length rises linearly with radius R ($U = 2\pi R$) while there is a quadratic increase for the leaf surface area ($A = \pi R^2$). Accordingly the decreasing air volumes towards the edges of the leaves have a larger influence on the

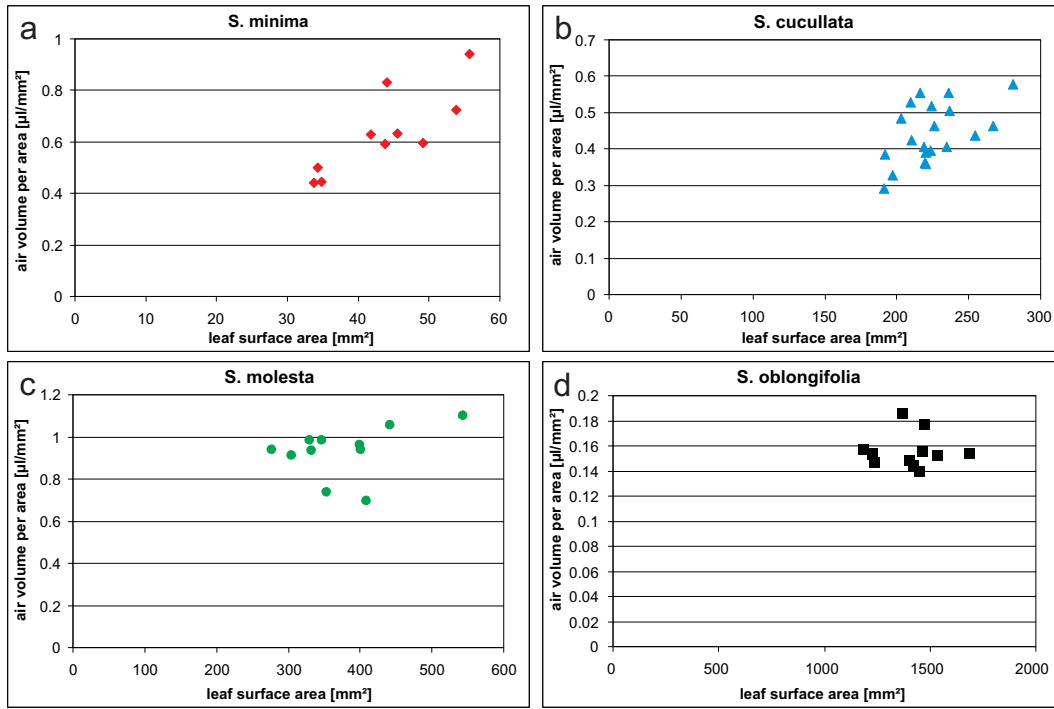


Figure 3.7: Air volume per surface area measured on four different *Salvinia* species. a) *S. minima* (n=10), b) *S. cucullata* (n=19), c) *S. molesta* (n=11), d) *S. oblongifolia* (n=12).

overall air volume on small leaves of *S. minima* and *S. cucullata* (Fig. 3.7a,b), than they have in species with larger leaves like *S. oblongifolia* (Fig. 3.7d).

Assuming a circular leaf (radius R) with a linear decline of the hair height H towards the edge for a width W specified for each species, results in an air layer in the shape of a truncated cone. The volume of this truncated cone represents the maximum theoretical volume V_{\max} of an air layer on a leaf with a given surface area and can be calculated to

$$V_{\max} = \pi \cdot H \cdot \left[R \cdot (R - W) + \frac{1}{3}(W)^2 \right] \quad (3.3)$$

Divided by the surface area this results in the mean air height. This should almost equal the hair height on the plants for an infinitely large leaf. Comparing these values for different leaf sizes with the values measured on *Salvinia* leaves (Fig. 3.8) shows a different result for the different species. For *S. minima* and *S. cucullata* the measured values are just slightly below the theoretically possible values. Those small differences might again be caused by the sagging of the air water interface between the hairs but also by the volume occupied by the hairs themselves. For *S. oblongifolia* and *S. molesta* the measured values range approximately 50% below the calculated values. *S. oblongifolia* hairs incorporate massive emergences that make up more than half of the hair height and grow closely to each other. They occupy a large portion of the space calculated before. Also all the trichomes grow inclined towards one side and are therefore easily bent down resulting in a thinner air film. There are two reasons for the lower air volumes on *S. molesta* compared to the calculated values. Firstly this species displays the lowest density of hairs compared to the other species. Because of this the air water interface is sagging much more in between the hairs and thereby reducing the air volume. *S. molesta* leaves also feature a different leaf form, which consist of two halves joined only in a

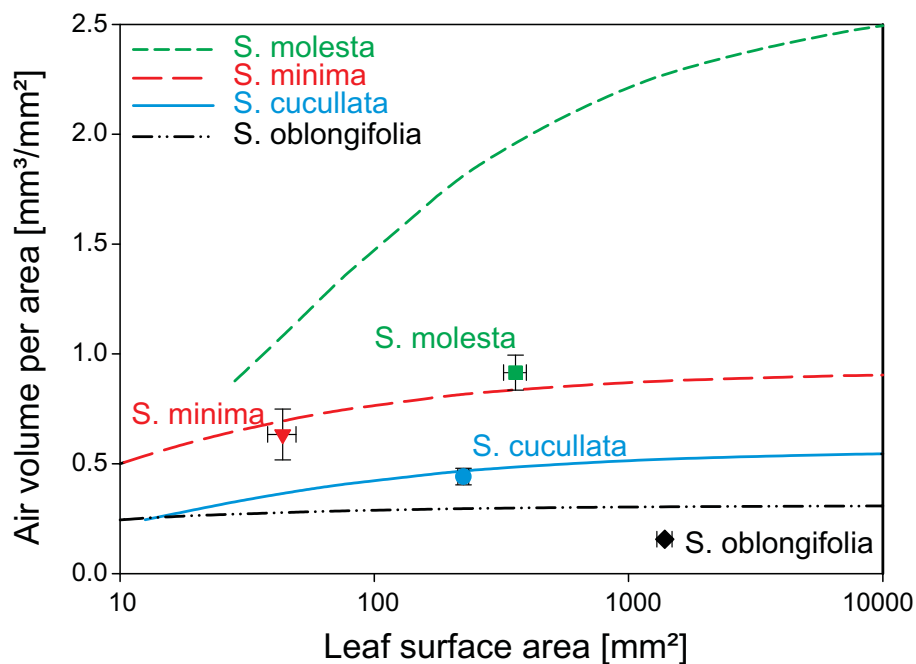


Figure 3.8: The air volume per surface area measured on 4 different *Salvinia* species compared to the theoretically possible values. (Symbols: median values, whiskers: 95% confidence interval, lines: theoretical maximum values)

small portion in the middle and having a rather pointed angle between them. Though the experiments were performed with care to prise the two halves apart, in a portion of the leaf surface near the joint the hair tips would interlink between each other and form an air pocket, which is considerably smaller than an air film with full height on those surfaces.

3.3 Conclusion

The presented method is a reliable way for measuring volumes of air layers on submerged superhydrophobic surfaces precisely. By adjusting the lever length of the needle the measurement range can be tuned appropriate to the air layer size. The method has been successfully applied to measure the air volumes on four different *Salvinia* species with their highly complex hierarchically structured surface, which hold up to 1 l/m^2 air under water.

As this setup can measure changes in buoyancy in real-time, it can also be used to monitor the change of air volumes over time, thereby giving an insight in the dynamic persistence of air layers and the progresses of their decrease. This knowledge can be fundamental for the creation of artificial surfaces with long-term air retention (e.g. for drag reducing ship coatings).

4 Long term air retention in *Salvinia*

Up until now the duration of air retention on *Salvinia* has only been visibly judged by the silvery shine of the air layer. But it has never been actually measured. There are also no data about the progress of air depletion. With the measurement setup described in the previous chapter it is now for the first time possible to monitor the air volume over time. This opens the possibility to measure the duration of air retention as well as the course of air loss.

4.1 Materials and Methods

In order to use the previously described setup for long term measurement a few change had to be made, because the strain gages used react extremely sensitive to temperature. In a measurement over time of the strain gage signal with a constant weight attached to the needle and the water temperature (Fig. 4.1) it is apparent, that fast temperature change affect the output severely. So to get a reliable buoyancy reading over longer periods of time a temperature control device for the setup had to be build.

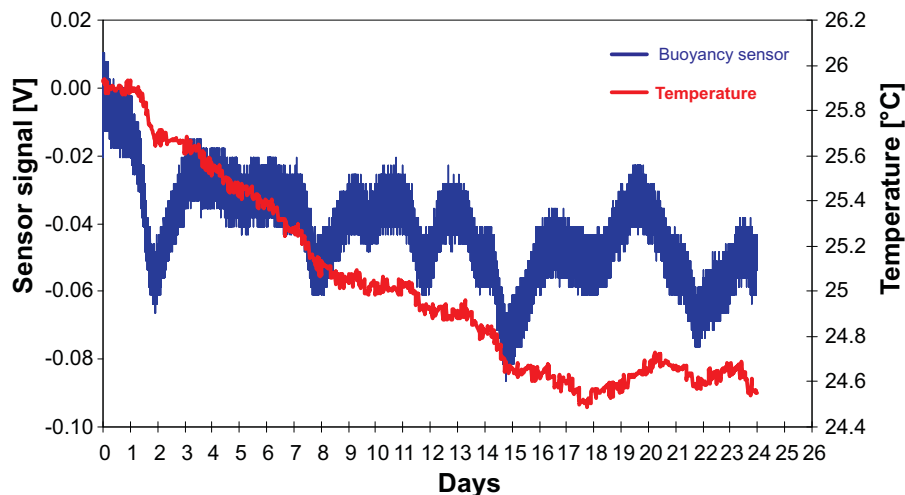


Figure 4.1: Temperature and sensor reading over time; temperature changes are effecting the buoyancy measurement

4.1.1 Temperature control

To achieve a constant temperature over time the aquarium in which the actual measurements was performed was placed inside a bigger aquarium (80×40 cm) filled with 30 l of water. This bigger container was covered on all sides with aluminum faced PUR insulation boards and two self-adhesive 320×137 mm heating films (*thermo Flächenheizungs*

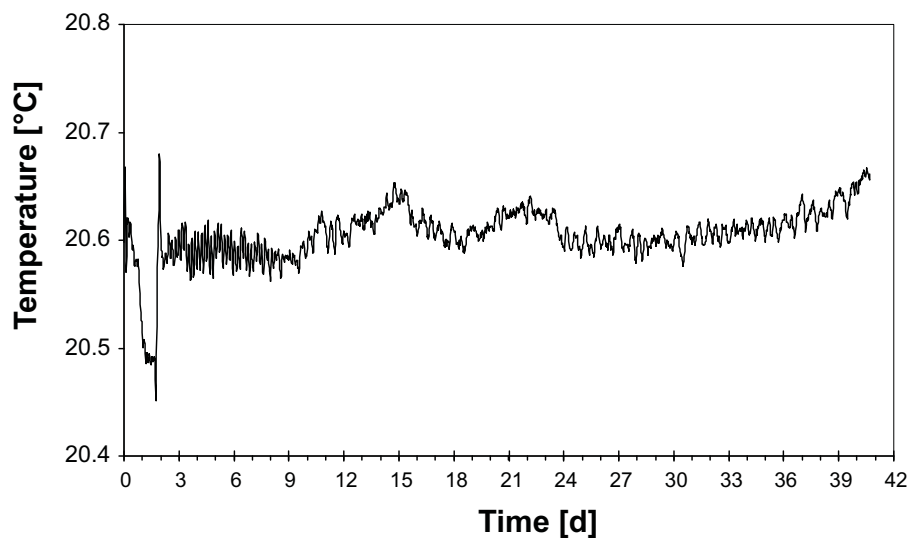


Figure 4.2: Temperature in the measurement setup with temperature control installed

GmbH, Rohrbach, Germany) were attached to the bottom. Those were connected in series to a power supply (Voltcraft EP-915, Conrad Electronic SE, Hirschau, Germany) at 15V and 2A and controlled by a PID universal controller (EUC442-230VAC-RS, SURAN Industrieelektronik, Horb, Germany) equipped with a thermal probe, which was placed at medium height inside the big aquarium.

Once leveled out this allowed a temperature to be stable at 20.6 °C with a tolerance of 0.1 °C (Fig. 4.2).

To compensate for other minor influences from the surrounding, an empty sensor was recorded with every measurement and its signal differences were subtracted from the actual measurement signal.

4.1.2 Aerenchyma of *S. oblongifolia*

Another modification had to be made to the measurement of *S. oblongifolia*. Compared to the other species examined *S. oblongifolia* has got a huge aerenchyma filled with air below its leaf (Fig. 4.3). While this air volume was not affecting the volume measurements in the previous chapter because only the leaf surface got wetted by water in the process, it got apparent after a long term submergence that the air stored in the aerenchyma does get replaced by water over longer periods of time. This results in a much bigger buoyancy reduction than only the air layer could cause. This gets obvious when taking the acquired volumes from the previous chapter as baseline and comparing it with the measured values (Fig. 4.4).

So to record only the differences in buoyancy from the air layer the aerenchyma needed to be cut off prior to measurement. This however led to an extremely fast decay of the leaf due to fouling processes at the cutting edge. To prevent this the cutting edges were sealed off by a sterilized 0.5% alginate solution that was then solidified by a short dip in 1% CaCl solution.

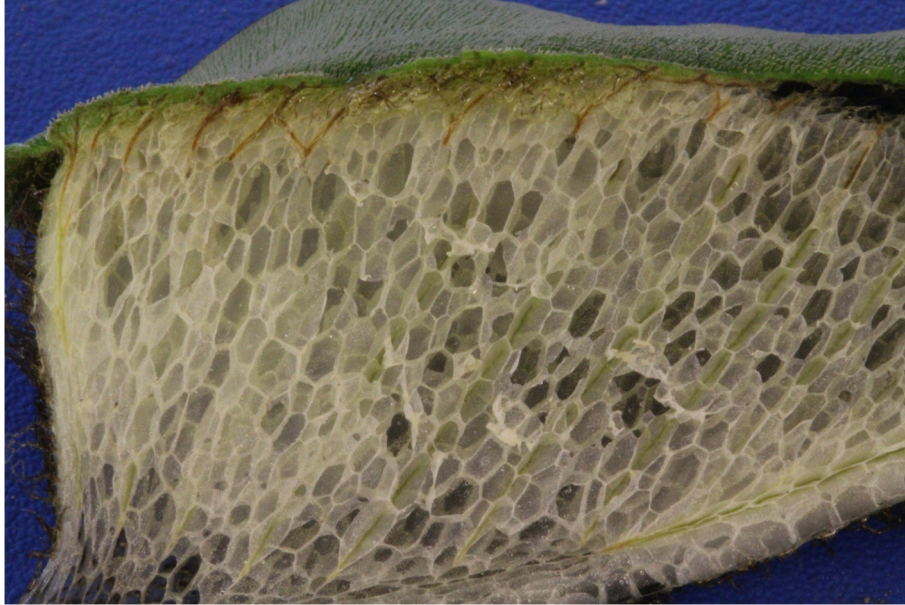


Figure 4.3: Section through a leaf of *S. oblongifolia*; the aerenchyma volume is large compared to the air retaining hairs on the upper leaf surface

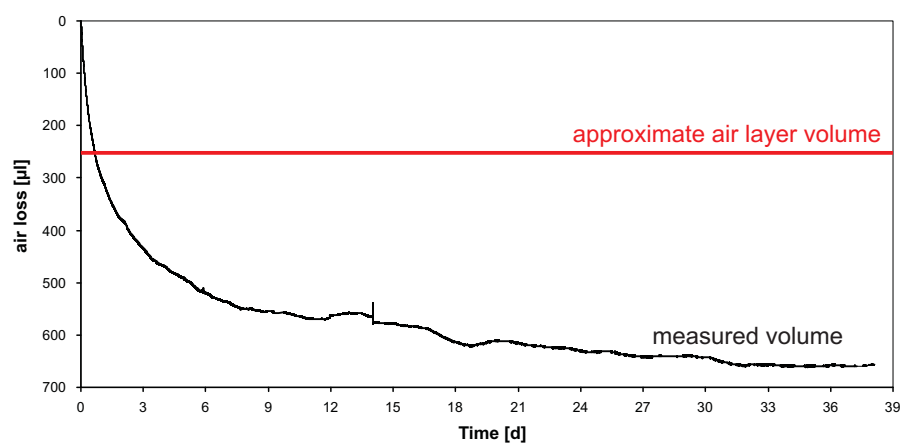


Figure 4.4: Measurement of air loss on *S. oblongifolia*; the measured air volume is higher than the theoretically possible air layer volume due to air being lost out of the aerenchyma as well

4.1.3 Measurement setup

For the measurement 5 sensors as described in chapter 2 were attached to the side of an aquarium ($30 \times 20\text{cm}$) which was filled to just below the sensors with water. This got placed inside the temperature control aquarium and given 2 days time to stabilize in temperature and gas concentrations. Fresh leaves of the selected four *Salvinia* species were each fixated to stripes of plastic by means of dental paste (President Light Body Gel, ISO 4823, PLB, Coltene Whaledent, Hamburg, Germany) and hung onto the bend of the needle of each sensor with 0.1 mm diameter nylon string. All samples were placed at the same water depth of approximately 8 cm. Small weights were attached to the string to compensate for initial buoyancy. One sensor was left empty for drift compensation.

The experiments ($n=8$) were performed in darkness to avoid influences of the light affecting the sensors and of photosynthesis. The forces were measured every 100 seconds until all air was depleted. States of leaf fitness and presence of air films were visually check in regular intervals.

4.2 Results and discussion

4.2.1 Progress of air volume changes

The readings of the buoyancy measurement depicts a distinct behavior for each individual *Salvinia* species. Figure 4.5 shows a typical sample graph for each of the four examined species.

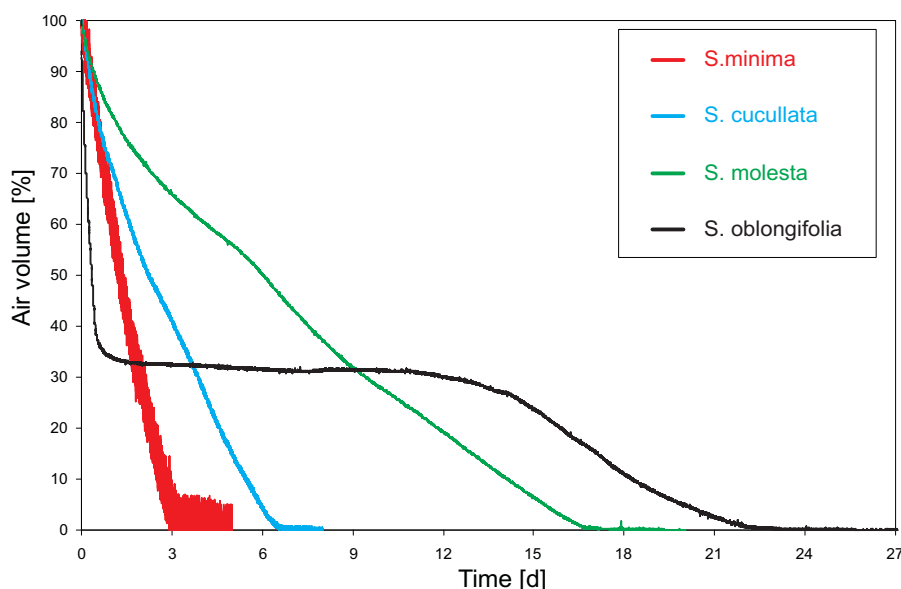


Figure 4.5: Comparison of the air decrease over time of different *Salvinia* species

While the curves of *S. cucullata*, *S. minima* and *S. molesta* display an almost linear air volume decrease until all air is depleted, the air layer of *S. oblongifolia* has a different progress of air loss. It decreases fast in the first one or two days and then stabilizes on a certain plateau. At this point an air layer is still visible on the leaves but it is not as

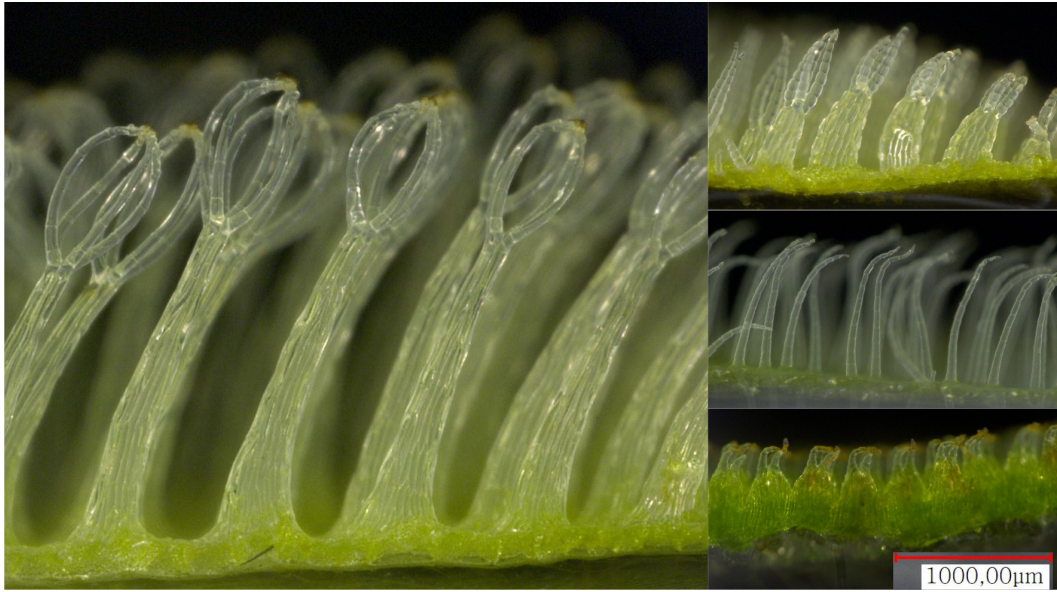


Figure 4.6: Comparison of the hair structures of a) *S. molesta*, b) *S. minima*, c) *S. cucullata* and d) *S. oblongifolia*

shiny as the initial air film. This plateau phase reaches its end, when the leaf is showing signs of withering and starts to become brown. After this the remaining air gets lost.

This different behavior can be explained by the shape of the hairs (Fig. 4.6). In contrast to the other species *S. oblongifolia* hairs grow extremely close to each other. Between their emergences there is not a nearly flat leaf blade surface. The emergences build rather a canyon like cleft network between them. Additionally the emergences themselves are of a dome like shape. Combined with the high contact angle of the surface this leads to a concave air water interface with little span width and a higher curvature. According to the Young-Laplace-Equation,

$$p_a = p_w + 2\sigma H,$$

this type of curvature (the mean curvature H is negative for concave air water interfaces) can reduce the pressure inside the air layer p_a relative to the water pressure p_w due to the impulse of the air water interface to reduce its area because of the surface tension σ [Konrad et al. 2009; Atkins 2006]. This prevents gas from diffusing into the water and causes *S. oblongifolia* to form a long term stable air film between its emergences. This air layer equals about 34.1 ± 8.6 percent of the initial air volume when freshly submerged. While the emergence takes up more than half of *S. oblongifolia*'s hair height (Table 3.1) the little volume in between the emergences compared to the bigger volume between the upper branches of the trichomes explains the 2:1 volume ratio of the plateau.

4.2.2 Rate of air volume changes

Looking at air loss right after submerging the leaves (Fig. 4.7), it is apparent that the rate of volume loss right after submergence displays significant differences between the different *Salvinia* species (Table 4.1). When divided by the leaf surface area the air loss rates are in the same order of magnitude (Table 4.1, Fig. 4.8). As diffusion is

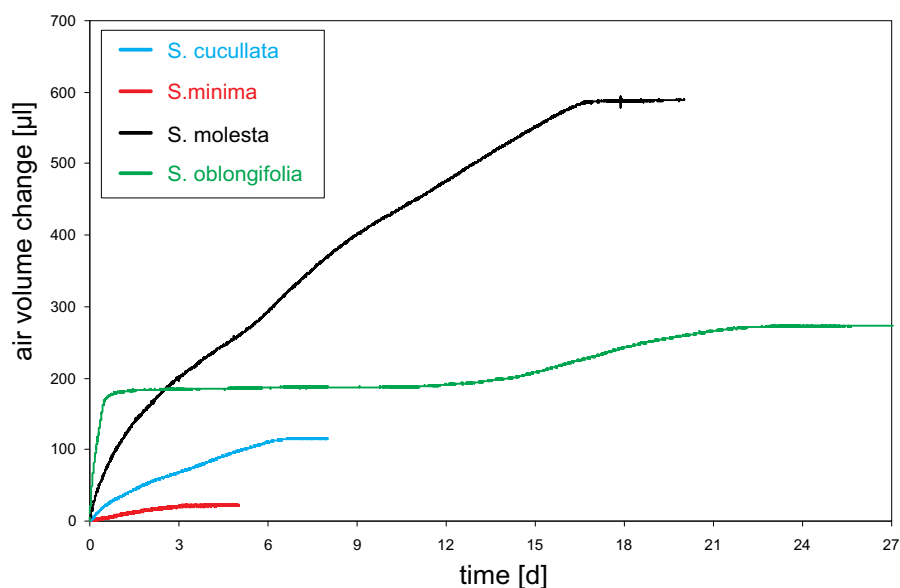


Figure 4.7: Measurement graphs of the changes of air volume over time on different *Salvinia* species

Table 4.1: Initial air loss of 4 selected *Salvinia* species ($m \pm s.d.$)

	air loss per time [ml/h]	air loss rate per area [$\mu\text{l}/\text{mm}^2 \cdot \text{h}$]
<i>S. cucullata</i>	3.3 ± 0.9	15.2 ± 4.3
<i>S. minima</i>	0.53 ± 0.17	10.2 ± 3.8
<i>S. molesta</i>	5.9 ± 1.2	9.3 ± 1.9
<i>S. oblongifolia</i>	28.8 ± 8.3	23.7 ± 5.3

proportional to the surface area [Atkins 2006], the dependency of air loss of the surface area implies that diffusion is the main factor of air loss. This is due to two factors: There is a higher pressure inside the air layer compared to the atmosphere because of the hydrostatic pressure. With the water in between as moderating medium the air inside the air film tends to diffuse towards the lower pressure of the atmosphere. A second reason is the metabolism of the leaf. As the experiments were carried out in darkness, there was no photosynthesis possible during the measurement. So the only metabolism the plant could perform was cellular respiration. This decreased the O_2 level in the air layer while increasing the CO_2 . Carbon dioxide has a much higher solubility in water than oxygen so it gets dissolved faster. This results in a higher partial pressure of nitrogen inside the air layer, which will also result in a faster diffusion of gas into the water.

4.2.3 Air layer persistence

The measurements also gave reliable data concerning the duration of air retention (Fig. 4.9). Due to its stable air layer on the level of the emergences *S. oblongifolia* displayed

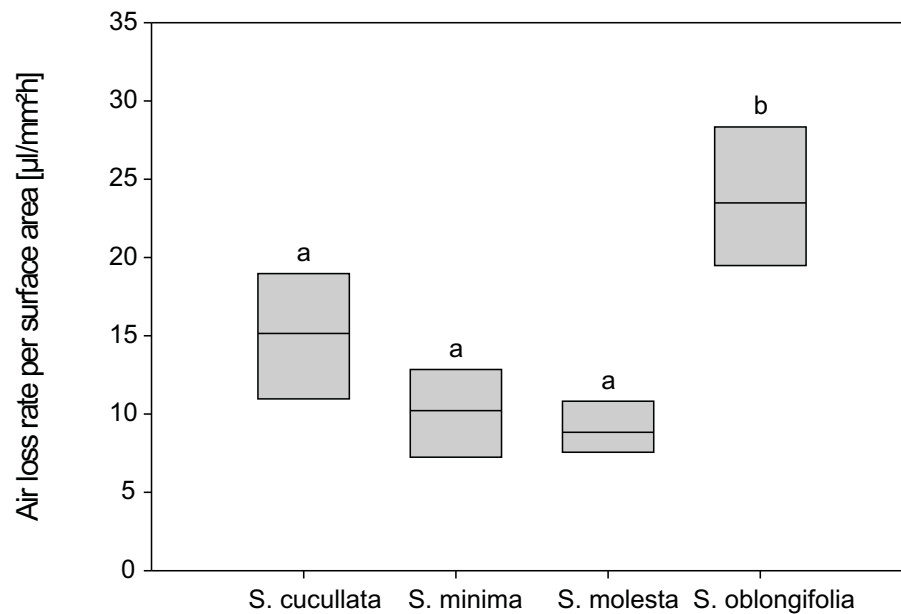


Figure 4.8: Rates of air volume loss per leaf surface area on different *Salvinia* species

a highly significant ($P < 0.001$ Holm-Sidak-Test) longer air retention than any other species. Leaf fouling processes caused the air to deplete after 31 ± 4 days. Despite the high rate of diffusion *S. molesta* also had a highly significant ($P < 0.001$ Holm-Sidak-Test) longer air retention than the remaining two species and lasted 15 ± 4 days. The large volume per surface area (Fig 3.8) compensated for this. *S. cucullata* (4 ± 2) and *S. minima* (4 ± 2) had quite similar air layer persistences. As explained before cellular respiration probably reduced the air layer persistence. So the duration of air retention measured here should be considered the minimum value and the air layer persistence on a technical surface with identical surface architecture and chemistry should be longer.

4.3 Conclusion

Summarizing the monitoring of the air layers of different *Salvinia* species revealed that long term air retention is possible. The emergences of *S. oblongifolia* shape the air water interface in a way that results in a pressure reduction inside the air layer and thereby keeping it stable. To extend air layer durability a high air volume with a low air water interface area is also beneficial. Under static circumstances diffusion is the main factor for air loss. This has to be counteracted in a technical application; e.g. shaping the air water interface (like on *S. oblongifolia*) or by adding gases with low solubility in water which changes the partial pressure of the natural gas components of air.

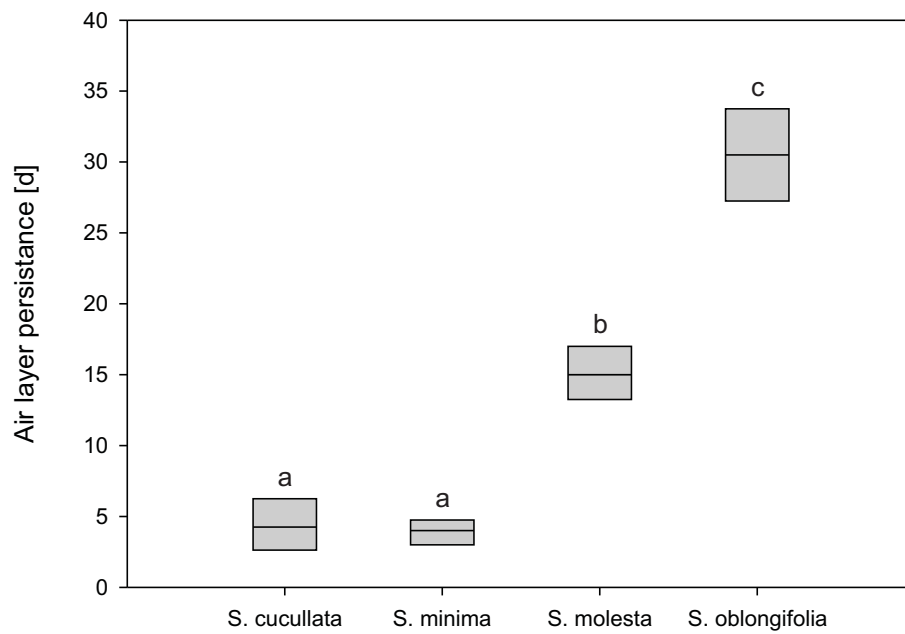


Figure 4.9: Measurement graphs of the changes of air volume over time on different *Salvinia* species

5 Stability of air layers under pressure fluctuations

For the application of air layers on ship hulls the air film does not only have to persist over long periods of time under static conditions. It has also got to withstand the stresses of turbulent flow and hydrostatic pressure. While the air layer stability under flow conditions gets examined by our cooperation partners of the chair for fluid mechanics of the University Rostock [Melskotte et al. 2012; Ditsche-Kuru et al. 2011b,a], here the stability under pressure conditions was examined.

There are two components leading to pressure on the ship hull. One factor is hydrostatic pressure. Due to the density of water the pressure increases by one bar for every 10m of depth. With a maximum loaded draft of current container ships of 12 meters Germanischer-Lloyd [2011] this results in a maximum hydrostatic pressure of 1.2 bar.

The other factors to pressure on ship hulls result from the dynamic water forces during cruise. Combined with the hydrostatic pressure those add up to a total maximum pressure of about 2.5 bar [Kaeding 2009]. However, the slamming forces, which occur in certain areas of the ship in high swell, can be much higher (up to 15 bar). But those occur only for very short periods of time and will therefore not be further investigated here.

5.1 Materials and methods

To research the effect of pressure on air layers, a setup had to be build that could pressurize a sample under water to at least these 2.5 bar while still being accessible to examination. This was achieve by building a pressure cell.

5.1.1 Pressure cell

The pressure cell consists of a PVC pipe crossing (TÜV rated to 10 bar) with 10 cm inner diameter, all four ends bolted with 2 cm thick disc by eight M8 screws (Fig. 5.1) and is placed upright with a 45° angle of all tubes. Both upper ends were covered with PVC discs; one gets removed for sample change, the other sports a connector for pressurization. Both lower ends were closed by acrylic glass discs. One of those gave access for illumination while the other served the purpose of sample observation by a camera. With the sample placed in the crossing at a 45° angle between the light source and the camera this architecture leads to a good visibility of the air film by reflexion (Fig. 5.2). The cell gets pressurized through a pressure reducer by helium, which has the lowest solubility of all gases in water [Greenwood 1997]. For safety reasons a relief valve limited the pressure to 6 bar.

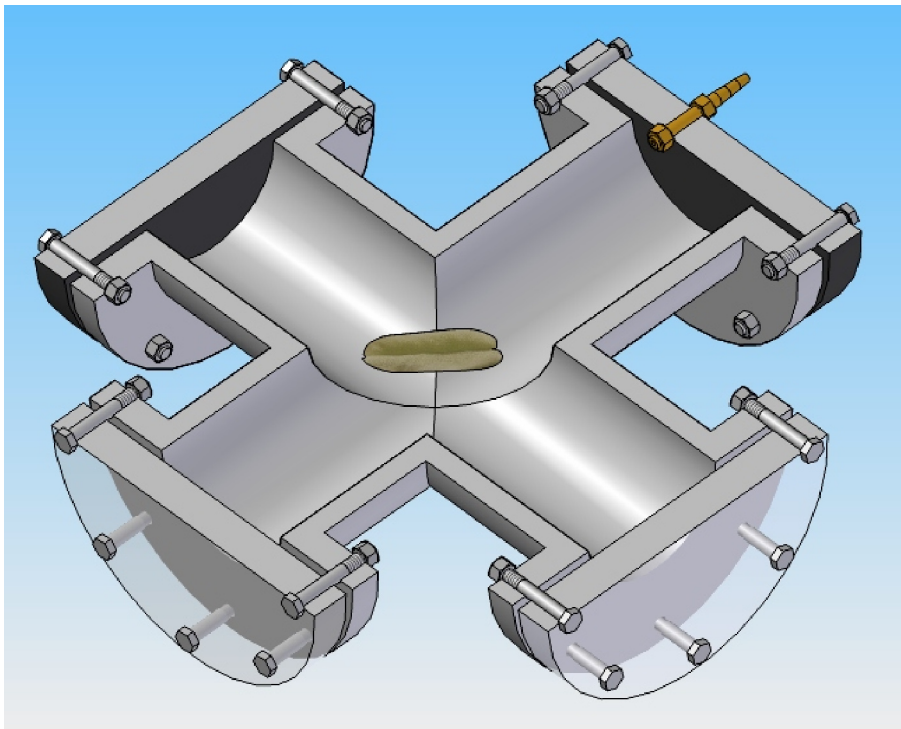


Figure 5.1: Scheme of the pressure cell; the air retaining leaf is positioned in the center of the pipe crossing, where it can be observed and illuminated through the transparent glass planes at the bottom. The system can be pressurized through the connector in the lid on the top right.

5.1.2 Measurement setup

Fresh leaves of the selected *Salvinia* species ($n=10$) get clamped on a custom designed holder and placed in the center of the pressure cell, which is filled to just above the crossing with water. For *S. cucullata* the scenario with an air bubble trapped in the leaf could be examined in this method as it did not interfere with the measurement like it did with the buoyancy setup. As this provided the more interesting results, it was the mainly used, but *S. cucullata* without the bubble of air was also examined with fewer repetitions. The leaves were being observed by a digital camera (Canon D550, Canon Inc., Tokio, Japan) equipped with a macro lens (Canon 60mm, Canon Inc., Tokio, Japan) and mounted directly in front of the viewing glass of the pressure cell. It was connected to a computer and remote controlled with EOS remote capturing software to prevent camera shake.

Pressure was slowly increased in 0.2 bar steps. An image was shot before the pressure was applied and for each step to be analyzed for air coverage on the leaf. Additionally videos of a pressurization were taken to examine the progress of air suppression. After 6 bar were reached the pressure was slowly released and a further image was taken at 0 bar for comparison with the initial air layer. The images were examined on the pressure at which water penetrated in between the hairs for the first time, the pressure at which no air layer was visible as well as the degree of restoration of the air layer after the pressure was released.

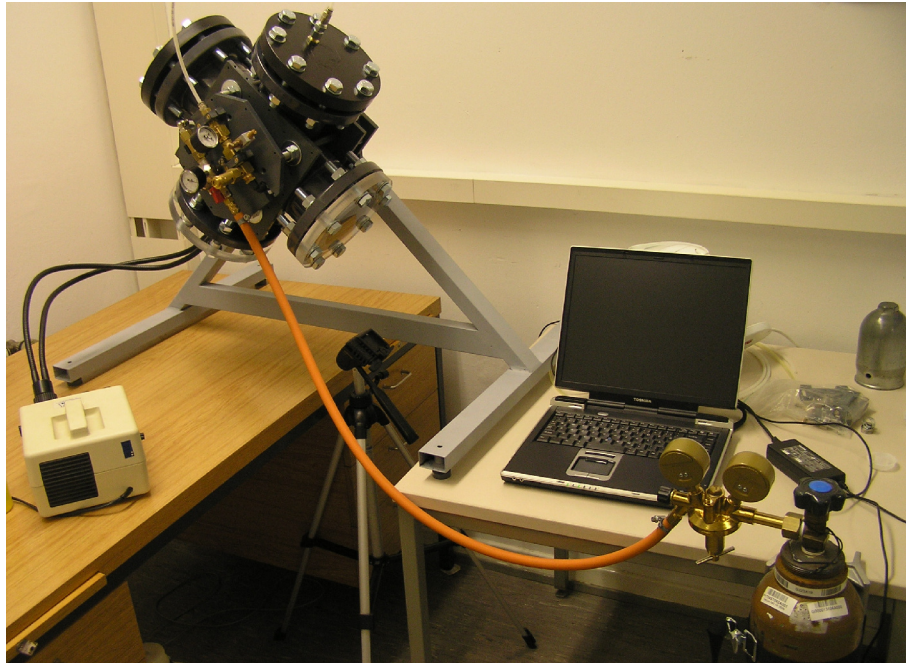


Figure 5.2: Setup of the pressure cell

5.2 Results

In general the air layers and their distribution on the leaf are much more difficult to analyze on the images than they were in direct observation, where different angles would help to distinguish the presence of air. Especially the changes in air coverage could be easily followed in real live. So the images in this section were interpreted with addition of real live observations.

5.2.1 *S. minima*

The air layer on *S. minima* (visible by the reflection especially on the lower leaf half in Fig. 5.3a) with the smallest air volume and its comparatively wide spaced hairs experienced the first penetration of water in between the trichomes at an average pressure of 0.3 ± 0.1 bar. The water would penetrate at the position with the widest gap between adjacent hairs. As the pressure increased the water moved horizontally through the trichomes towards the leaf edges, but left a small bubble of air trapped between the four branches of each trichome (white spots in Fig. 5.3b). At 2.2 ± 0.3 bar most of the air in between the trichomes got suppressed by water (Fig. 5.3c). The air bubbles between the branches got smaller with increasing pressure and vanished at an average pressure of 5.2 ± 0.8 bar (Fig. 5.3d).

While slowly lowering the pressure from 6 bar (Fig. 5.3e) the air layer progressively reformed. However, it did not reach its original extend. Though difficult to distinguish in Fig. 5.3f, the air layer reformed on some parts of the leaf while other stayed wetted. In some cases air was lost in form of air bubbles as the pressure decreased. On average $76 \pm 16\%$ of the leaf surface were covered by air after depressurization.

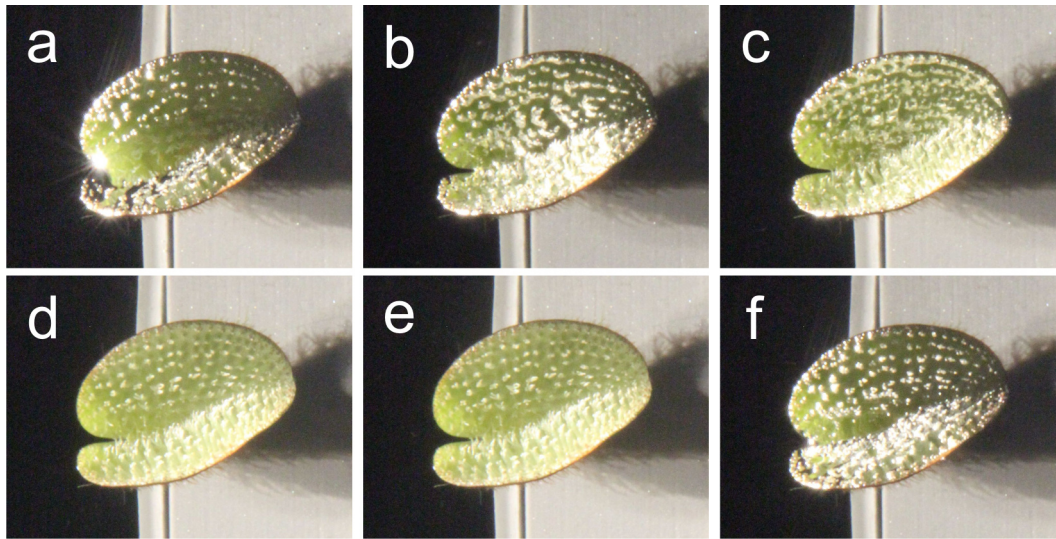


Figure 5.3: Air layer on *S. minima* during a pressurization cycle, a) 0.0 bar, b) 0.6 bar, c) 2.0 bar, d) 5.0 bar, e) 6.0 bar, f) after depressurization to 0.0 bar

5.2.2 *S. molesta*

On *S. molesta* the first 'break in' of water between the hairs already appeared at an average pressure of 0.12 ± 0.04 bar (Fig. 5.4b). Like on *S. minima* the water subsequently spread through the trichomes from the first point of penetration and air bubbles got trapped in the baskets of the egg beater hairs (Fig. 5.4c). At approximately 3.6 ± 0.7 bar all areas in between the trichomes were filled with water (Fig. 5.4d). Following this the trapped air bubbles got smaller and at an average pressure of 5.8 ± 0.3 vanished (Fig. 5.4e). In some cases several air bubbles lasted till the maximum pressure of 6 bar.

On depressurization the reformation of the air layer started at the leaf edges, where the hair structures are lowest and densest. Again the loss of air bubbles could be observed in some cases while not all of the air layer was reestablished (Fig. 5.4f). After depressurization $81 \pm 10\%$ of the area was covered by air on average.

5.2.3 *S. oblongifolia*

Upon compression the air layer of *S. oblongifolia* displayed a more homogeneous behavior compared to the previous two species. The air water interface moved towards the leaf either uniformly or in large patches instead of moving through the trichomes horizontally. Like in the long term stability tests of the previous chapter a two step process could be observed. First the air got pressed towards the leaf at 0.27 ± 0.1 bar (Fig. 5.5b). Then the reflectivity stayed quite similar at further pressure increase (Fig. 5.5c) before the air would also disappear between the trichomes at 1.2 ± 0.2 bar (Fig. 5.5d). As the pressure kept rising the green of the leaf got more intense up to approximately 3 bar (Fig. 5.5e).

Lowering the pressure from 6 bar reformed the air layer only in small portions of the leaf ($31 \pm 25\%$) while a lot of air was visible as air bubbles on the leaf surface (Fig. 5.5f). Starting the depressurization from 3 bar led to a similar result.

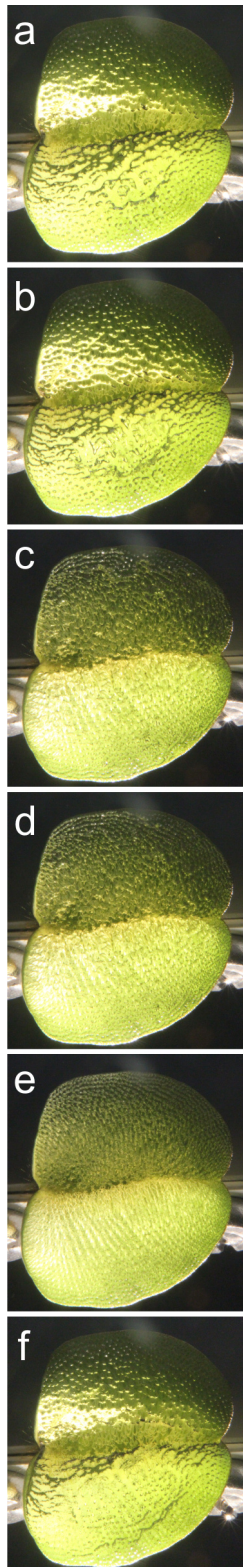


Figure 5.4: Air layer on *S. molesta* during a pressure cycle, a) 0.0 bar, b) 0.1 bar, c) 3.0 bar, d) 4.0 bar, e) 6.0 bar, f) after depressurization to 0.0 bar

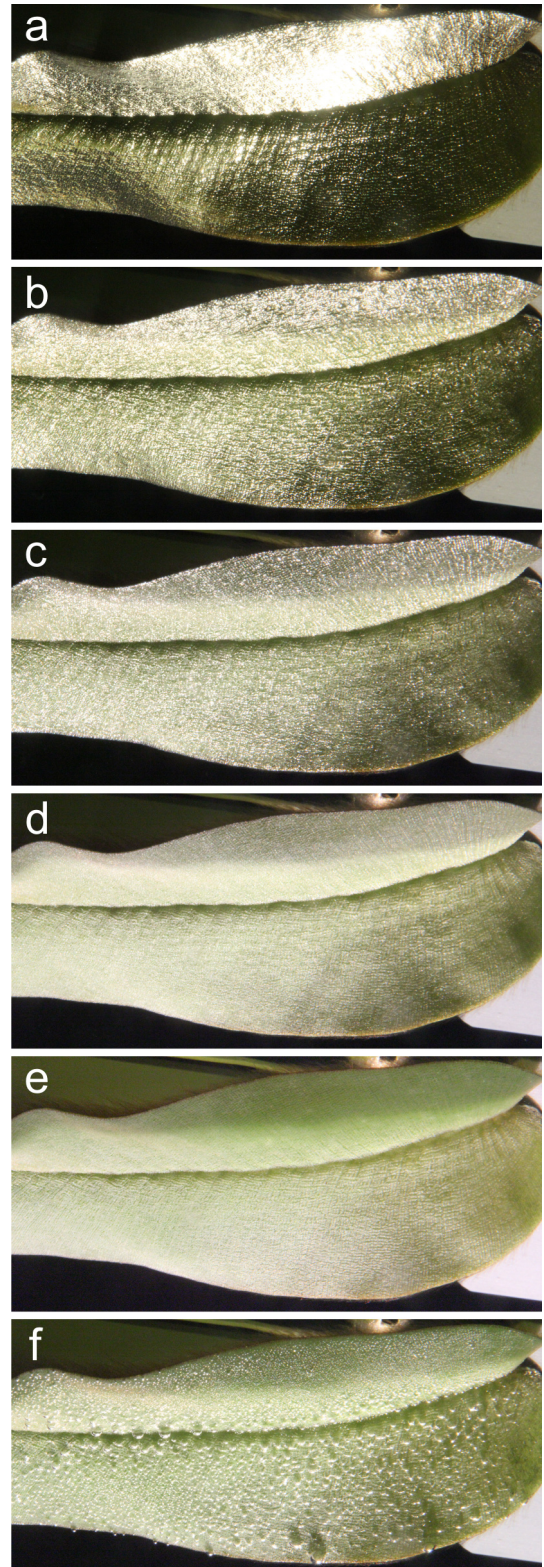


Figure 5.5: Air layer on *S. oblongifolia* during a pressure cycle, a) 0.0 bar, b) 0.2 bar, c) 0.8 bar, d) 1.2 bar, e) 6.0 bar, f) after depressurization to 0.0 bar

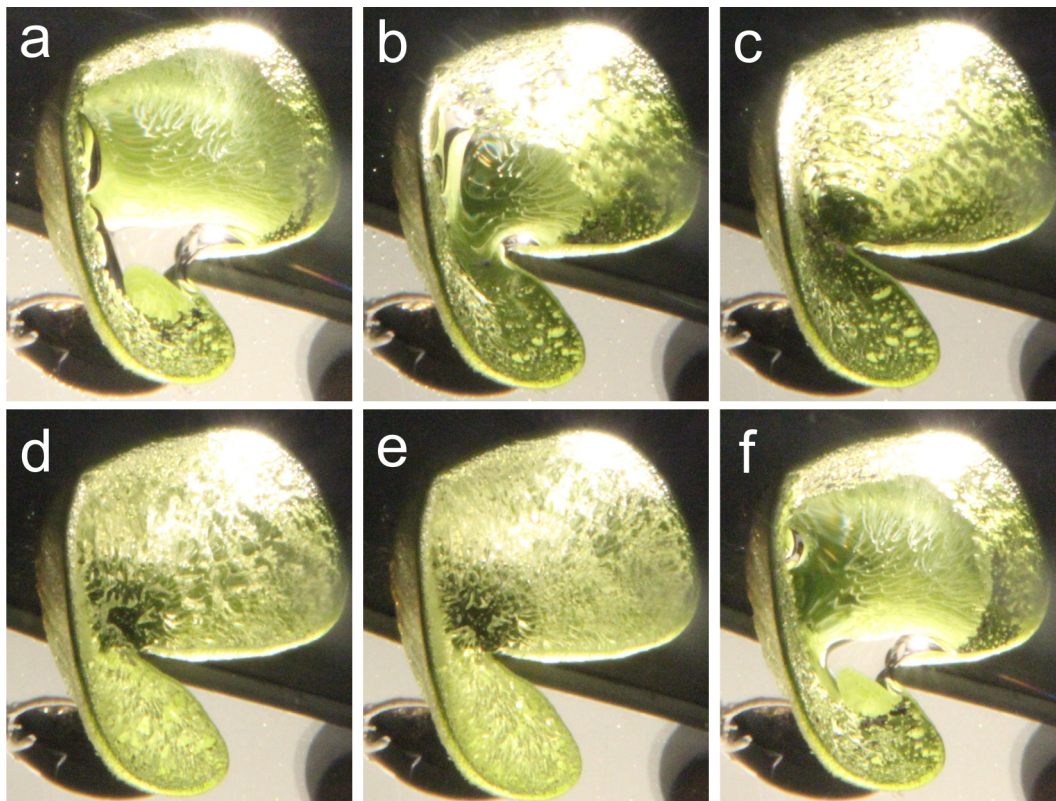


Figure 5.6: Air layer on *S. cucullata* during a pressure cycle, a) 0.0 bar, b) 0.6 bar, c) 1.0 bar, d) 3.0 bar, e) 6.0 bar, f) after depressurization to 0.0 bar

5.2.4 *S. cucullata*

In this experiment *S. cucullata* represents a special case compared to the other species. Due to its hood shaped leaf, *S. cucullata* is capable of trapping an air bubble inside its leaf (Fig. 5.6a) rather than an air layer supported by the hairs.

If examined like in the previous two chapters without the air bubble (further abbreviated as '*S. cucullata*-') it performed pretty similar to *S. minima* but instead of air getting trapped between the branches of the trichomes some air got trapped between larger clusters of trichomes. Also the penetration of water between the hairs happened at several places simultaneously so that there were larger patches wetted at once. The first 'break-in' appeared at 0.27 ± 0.12 bar ($n=3$) and no air visible between the trichomes was achieved at 5.3 ± 1.2 bar. The depressurization led to an average air covered area of $53 \pm 21\%$.

With an air bubble inside the hood shaped leaf *S. cucullata* (further abbreviated as '*S. cucullata*+') performed differently. This air bubble provided a volume of air to be depressed to an air film between the hairs when increasing the pressure (Fig. 5.6b). Accordingly the first penetration of water in between the hairs occurred at a higher pressure of 0.8 ± 0.3 bar (Fig. 5.6c). Afterwards the air would slowly indent at several spots while larger areas keep the air (Fig. 5.6d). Only in a few cases there was no air visible at 6 bar (Fig. 5.6e).

During the release of the pressure the air first reestablished an air layer on the hairs before reforming the air bubble inside the leaf (Fig. 5.6f). In some cases air bubbles escaped the leaf during depressurization, but generally the regeneration rate was quite high ($94 \pm 9\%$).

5.3 Discussion

5.3.1 Comparison of the pressure resistance

Taking the pressure at which water penetrates in between trichomes as a benchmark, three species are quite equal with two scenarios sticking out. While *S. minima*, *S. oblongifolia* and *S. cucullata-* all range slightly below 0.3 bar, *S. molesta* and *S. cucullata+* display a significant difference (Fig. 5.7).

For *S. molesta* the lower resistance against pressure can be explained by the longest hairs and the lowest trichome density of all the species. A slight bending of the leaf can lead to a rather big gap between two adjacent hairs. This gap provides a weak point in the resistance against water penetrating the air layer.

S. cucullata+ with its large reservoir of air held by the leaf shape instead of the hairs encounters the situation of air pressing against the tips of the hair only after the air has been sufficiently compressed for its volume to just fill the space between the hairs.

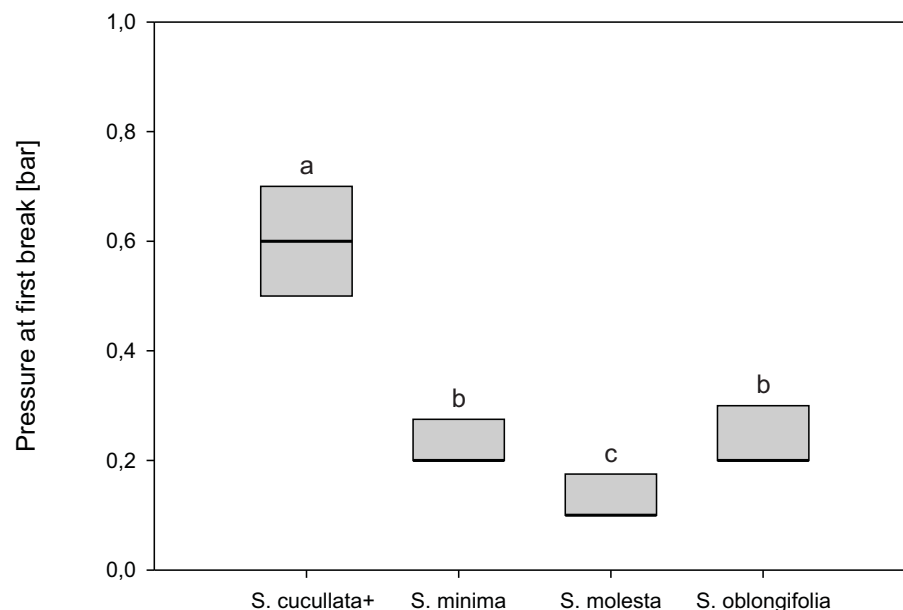


Figure 5.7: Pressure at which water penetrated between the hairs of different *Salvinia* species (n=10)

S. oblongifolia is the only species, which is not capable of retaining at least a minimal amount of air in between the trichomes at the pressures experienced on a ship hull (2.5 bar) [Kaeding 2009]. Fig. 5.8 shows clearly that its ability to maintain air is significantly lower compared to the other species. Because of its small air volume per surface area the air gets compressed enough to just cover the surfaces as a thin layer held up by the wax

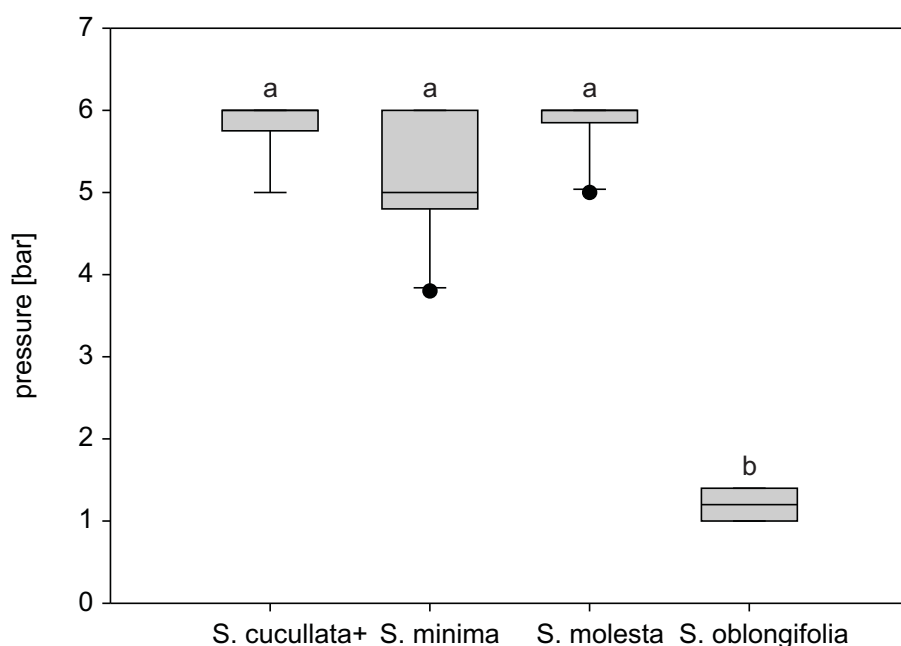


Figure 5.8: Pressure at which no air is visible between the trichomes of different *Salvinia* species (n=10)

crystals at approximately 1.2 bar. This air layer also collapses partially as the pressure reaches 3 bar.

However, an other cause for the comparatively low performance under pressure of *S. oblongifolia* is the larger aerenchyma. Even though most of it was cut off and the cuts sealed by sterilized 0.5% alginate solution like in the previous chapter, the aerenchyma of *S. oblongifolia* is still larger than those of the other species; especially when compared to the air volume held by the hairy surface structures.

The experiments also revealed that surfaces with a higher hair density (like *S. oblongifolia* and *S. cucullata*) experience a more uniform depression of the air layer while the lower densities of the other species led to local failures which could then spread horizontally through the hairs. Which kind of failure will be better in the practical application of drag reduction has to be researched in further test in the flow channels of our partners at the chair of fluid mechanics in Rostock.

5.3.2 Regeneration of the air layer after depressurization

The regeneration of the air layers works obviously best, if the surface has not been wetted during the pressure cycle (Fig. 5.9). Thus a high volume per surface area is beneficial for the restoration. *S. oblongifolia* has the lowest hair structures and accordingly the lowest volume per surface area (Fig. 3.6). This leads to water wetting even the nano structure of the wax crystals (at least partially) and the surface being wetted in the Wenzel-state. This gets apparent by a more intense green color of the leaf surface at pressurizations to 3 bar and above. A reformation of a Cassie-Baxter-state after depressurisation is thereby prevented [Quééré et al. 2003]. The high volumes of *S. cucullata+* and *S. molesta* prevent a full Wenzel-state even if compressed by 6 bar overpressure. So the regeneration rate is much better. Additionally the air trapped in the baskets of the egg beater hairs act

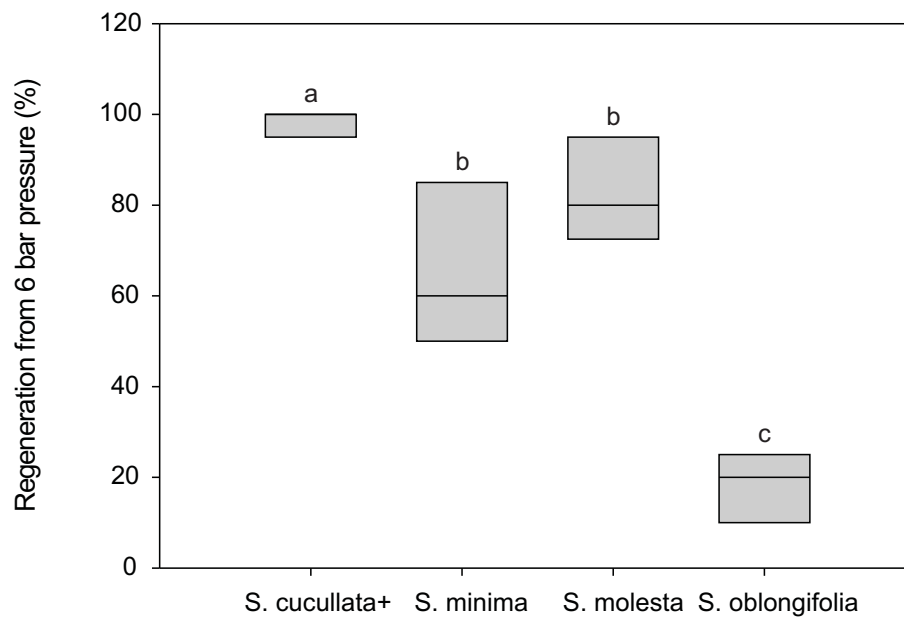


Figure 5.9: Percentage of air layer regeneration on different *Salvinia* species after lowering the pressure from 6 bar to ambient pressure (n=10)

like a magnet to the air water interface. As soon as the interface rises enough to touch this air bubble, the interface immediately jumps to the tip of the hairs. The smaller air water interface between the hair tip is energetically favorable to the sum of the interfaces of the air bubble in the basket and the interface between the basket.

5.4 Conclusion

The pressurization experiments revealed that high air volumes per surface area are advantageous to retain at least a partial Cassie-Baxter-state under pressure, which also helps the restoration of the air layer after depressurization. Closed loop structures like the baskets at the top of the egg beater hairs also help setting the air layer back to its original level at the tip of the hairs by trapping air bubbles in them.

6 Technical surfaces for air retention

For the transfer of the air retaining properties into technical applications there are several possible methods. One could be the Flock technique which generates a dense cover of textile fibers. It is widely applied in several industries (door seals in cars, imprinting on textiles or refinement of surfaces) and its generates highly stable surfaces which can withstand demanding conditions like dish washers or the wear on carpets. It has also been applied on the nets of aqua farming nets as an anti fouling measure (though without an air layer) [Breuer 2010] and has proven to last in marine environments.

6.1 Flock surfaces

The flock technique generates a hairy surface by shooting small textile fibers (called flock) in a thin layer of glue. To achieve this the fibers possess a coating that separates charges. This causes the flock to orient vertically in a high voltage electrical field before being accelerated towards an electrode. So in the flocking procedure the substrate with previously applied glue is earthed while the flocking machine is negatively charged. Flock fibers brought into this electrical field bounce up and down in the electrical field until they get stuck in the glue layer on the substrate. Due to the stochastic process of getting stuck in the glue the orientation of the flock fibers is not strictly vertical. Any orientation between 0° and 90° is possible, but with a tendency towards a vertical orientation because of the electric field [Lake 2009].

In a first attempt to apply the principals found on *Salvinia* Flock samples were generated in cooperation with our industrial partner SwissFlock Inc. (Branch Germany, Stuttgart). As the form of the flock fibers matches best with the hairs of *S. cucullata*, their structural parameter were used as orientation to design the flock surfaces.

6.1.1 Materials and methods

The flock technique can not control the density of the hair application. The surface gets filled until the bouncing fibers do not get in touch with the glue any more. So we used a different approach to set the hair density on our surfaces. We used a mixture of very short, white (0.3 mm) flock fibers with black fibers of our target hair size for flocking. The short fibers would occupy the place in between the bigger hairs and create a kind of 'undergrowth' similar to surface structure on the elytra of *Notonecta glauca* (Fig. 6.1). By adjusting the ration between short and long flock the density on the fabricated surface could be controlled.

For testing the parameters hair height, hair thickness and density were separately varied approximately by the factor two in both directions from a reference sample leading to seven different surfaces (Table 6.1). Additionally one surface with the densest possible

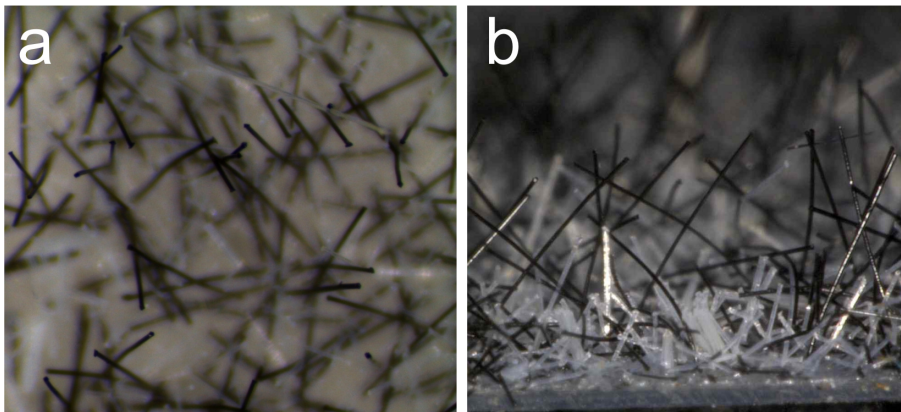


Figure 6.1: Sample of flock surfaces with sparse, black, long fibers in a dense cover of short, white fibers; a) top view, b) side view

Table 6.1: Structure parameters of the flock samples used

Flocksample	Density [1/mm ²]	Length [mm]	Diameter [μ m]	Aspekt ratio
1 (Reference)	9.4	0.75	19	39
2	21.1	0.75	19	39
3	35	0.75	19	39
4	13	1.2	19	63
5	10.1	0.75	50	15
6	13.6	0.5	19	26
7	13.6	0.8	10	80
Antifouling	17.8	3	70	43
'Undergrowth'	na	na	na	

cover of the 'undergrowth' and a surface with the flock used for anti-fouling measures by Breuer [2010] was included in the test.

All flock surfaces were hydrophobically coated in a two step process. First they were sprayed with Antispread (F2/200 Fluorcarbon 60, Horb-Ahldorf, Germany) leading to thin film on the substrate. After drying (approximately 1 hour) Tegotop 210 (Evonik Degussa GmbH, Germany) was applied by an air brush tool to form a hydrophobic nano structure.

Eight samples (3x3 cm) of each surface were glued in random order onto a pane of acrylic glass which was weight down with lead weights to compensate for the buoyancy of the air films.

This pane of acrylic glass was then submerged in an aquarium at a water depth of 15 cm and illuminated from a 45° angle (Fig. 6.2). A red plastic shield was placed at the rear side of the aquarium for easier detection of the reflections on the air layers. Pictures were taken automatically every 3 hours by a digital camera (Canon PowerShot SX10, Canon inc., Tokio, Japan) tethered to a computer. The duration of air retention was determined by tracing the silvery reflexion of the air layer on the photographs.

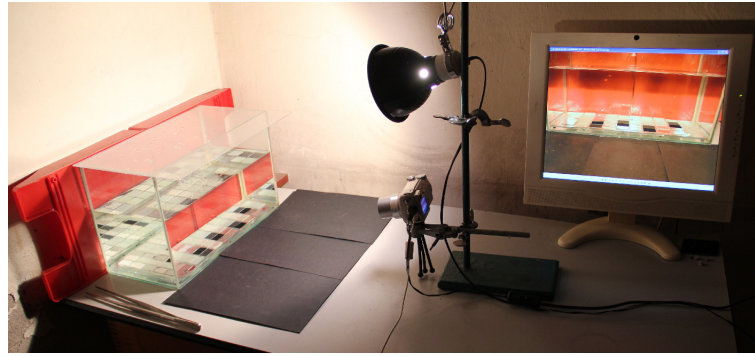


Figure 6.2: Recording setup for air layer persistence testing on flock surfaces

6.1.2 Results and discussion

The submerged flock samples showed prolonged air retention and revealed different effects of their surface parameters on air layer stability (Fig. 6.3).

Density

Increasing densities prolonged the duration of air retention (Fig. 6.3a). There was a highly significant ($P < 0.01$) increase in air layer persistence of both samples with higher densities (green bars in Fig. 6.3a) compared to the reference (blue bars in Fig. 6.3a). Between the two surfaces with higher densities there is not a significant difference, though a slightly better air retention and lower tolerance of the sample with the highest density is visible. Higher densities of hairs increase the area of support for the water and decrease the distance over which the air water interface has to span. This improves the counterforce against the water penetrating between the hairs and thereby stabilizes the air layer.

Diameter

The different hair diameter revealed no significant differences (Fig. 6.3b). The reference had a slightly lower air layer persistence (9.8 ± 4.0 days) than both the sample with lower (red bars in Fig. 6.3b, 13.2 ± 4.0 days) and the one with higher diameters (green bars in Fig. 6.3b, 11.6 ± 3.3 days).

Length

Both samples with differing hair length had a significantly ($P < 0.05$ Holm-Sidak-Test) longer air retention than the reference sample (Fig. 6.3c). From the experience with the natural surfaces of *Salvinia* a higher air layer persistence was to be expected, as the diffusion would take longer with the higher volume of the longer hairs. Taking the 'anti-fouling-flock' into account the results match the expectations much better, with the longest hairs having a highly significant ($P < 0.001$ Holm-Sidak-Test) longer air retention than all other samples. Having a closer look at the surface with the shortest hairs reveals the reason for the longer air retention compared to the reference. The height difference between the test hairs (0.5 mm) and the 'under growth' (0.3 mm) is too small. Due to the

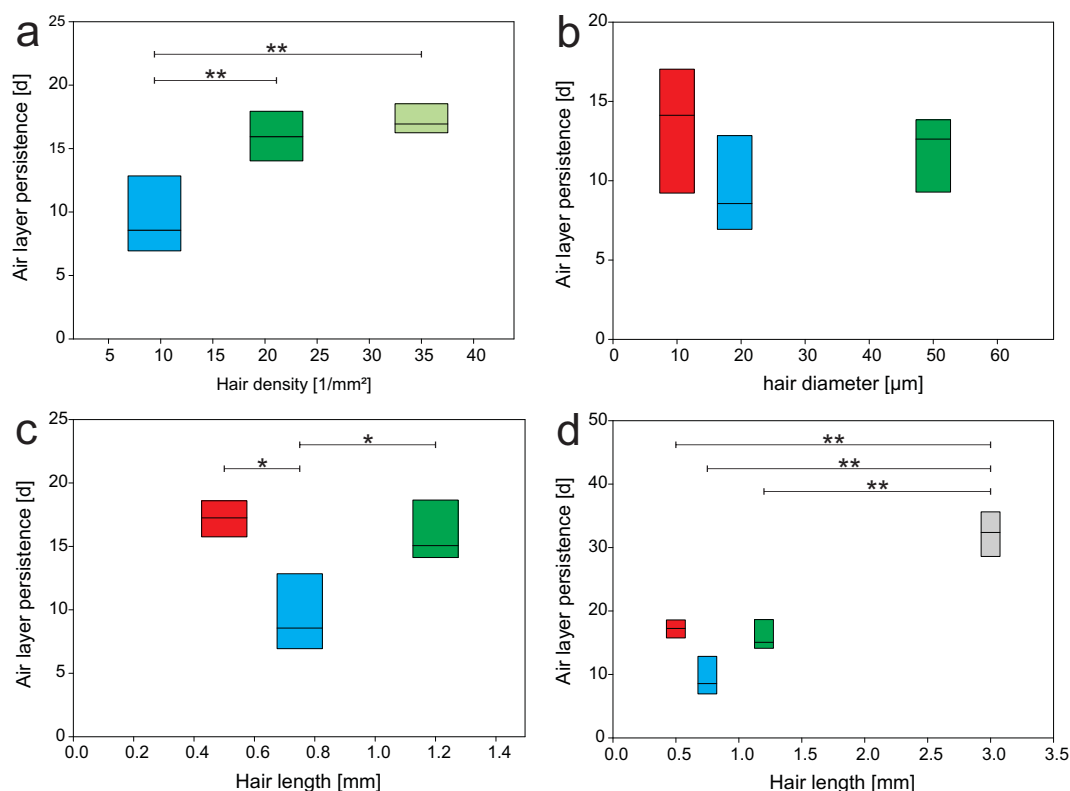


Figure 6.3: Air layer Persistence on flock surfaces with different a)hair densities, b)hair diameters, c,d) hair length; blue bars: reference samples, green bars: higher values, red bars: lower values; median values and 95% confidence intervals (n=8)

stochastic orientation of the flock they form a continuous height range between 0.3 and 0.5 mm resulting in a surface with a mean height of 0.4 mm and much higher density. This leads to a longer air retention than the reference. So taking this sample out of the calculation the expectation of longer hair leading to larger air volumes and resulting in a longer air retention got met.

6.2 Artificial Salvinia-effect surface

Our cooperation partner from the KIT succeeded in creating the first technical air retaining surface with Salvinia[®]-effect (hydrophilic tips on superhydrophobic structures). This enabled us to study its effect on air retention in detail without the influences and variations of the biological material. The advantages of the hydrophilic pins in turbulent/low-pressure conditions has previously been described and tested [Barthlott et al. 2010]. It is however unknown if and how these hydrophilic tips effect the long term stability of the air layer under static conditions. The new technical surfaces allow for the first time to investigate this long term stability.

6.2.1 Materials and methods

Two different sample sets were made. The surfaces consist of a quadratic array of pillar structures with an area of 20mm^2 on the smaller sample and 145mm^2 on the bigger sample. While one sample each was completely superhydrophobic the structures of the other samples got a hydrophilic dot on each tip to make them hydrophilic (Gandyra & Schimmel, unpublished).

Both samples were fixated on slings of 0.1 mm thick nylon cord with superglue (UHU Sekundenkleber, UHU GmbH, Bühl, Germany) and attached to the buoyancy measurement setup described in chapter 2. As previously described buoyancy measurements were recorded every 100 seconds until all air was depleted.

6.2.2 Results and discussion

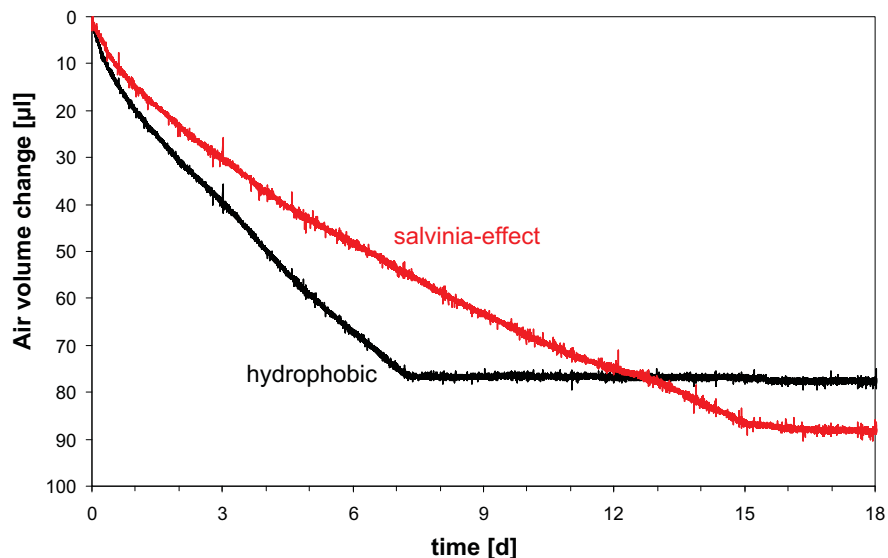


Figure 6.4: Comparison of changes in air volume on the smaller samples; one completely hydrophobic and one with hydrophilic tips on the hydrophobic structures (*Salvinia*[®]-effect)

The readings displayed a similar behavior for both the small (Fig. 6.4) and the big sample (Fig. 6.5). In both cases the samples with hydrophilic tips had a lower rate of air loss and a longer duration of air retention. Apparently the hydrophilic tips do not only improve the stability of air layers under pressure fluctuations, but also improve the long term stability under static conditions. One reason for this might be a fixation of the water edge at the boarder between the hydrophilic and hydrophobic surface on the structures. This could lead to a more concave shape of the air water interface. Due to the such induced lower pressure inside the air layer compared to the hydrophobic sample the diffusion responsible for the reduction of air could be slowed down. However, a confusing fact lies in the bigger air volumes measured on the *Salvinia*[®]-effect samples. Because of the different initial shape of the air water interface one would expect the entirely hydrophobic sample to maintain the higher air volume. Maybe this was just coincidence as all samples are individually produced and might have slight differences. Unfortunately there was only one measurement possible with each sample and there were only very few

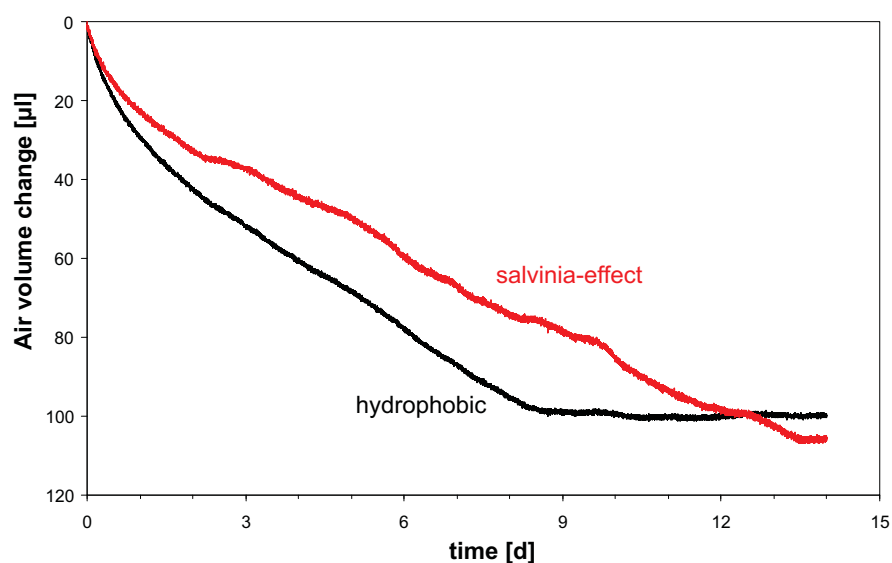


Figure 6.5: Comparison of changes in air volume on the bigger samples; one completely hydrophobic and one with hydrophilic tips on the hydrophobic strictures (Salvinia[®]-effect)

samples, because they are quite time-consuming in production. So further repetitive measurements have to be performed to validate the results and clarify the difference in measured air volume.

6.3 Replication

As described by Solga et al. [2007] one of the key factors to air retention are cavities. Though there are different ways to achieve simple forms of cavities in mass production like textile loops (Velcro[®]), more complex cavities are expensive and slow to produce. Methods for those include rapid prototyping techniques like selective laser sintering (SLS), fused deposition modeling (FDM) or stereolithography (SLA). As the previous experiments demonstrated a more complex form of the air retaining structures like the egg-beater-hairs are beneficial for a stable air retention. Therefore a cost efficient method for the production of large areas of air retaining surfaces is necessary.

Biological surfaces have previously been transferred into technical materials for studying by a replication technique [Koch et al. 2008b] which has also been use in chapter 2 for the replication of structured wafers. This method allows only for small and simple cavities and is not capable of producing 'closed loop' structures like the egg-beater hairs of *S. molesta*. So in order to produce large quantities of custom designed surfaces build by rapid prototyping I attempted to modify the existing replication technique for this application in cooperation with Dipl.-Biol. Adrian Klein. The aim was to generate 'closed loop' structures with just basic requirements for precision (rather μm scale opposed to the nm scale precision described by Koch et al. [2008b]).

In order to replicate such complex structures it was necessary to find a negative molding material that would allow to remove the template and close the cuts occurring after the withdrawal of loops, while leaving the form of the template open. Agarose gel as

frequently used in molecular biology displays such behavior. Due to the high water content and a fluidity controllable by the temperature it reseals small cuts instantly while being able to adapt to any form of its surroundings.

6.3.1 Materials and methods

Surfaces for replication

Fresh plant material of *S. molesta* was used as a biological template to test the replication technique. Additionally our cooperation partners from the KIT generated a sample with 25 mechanically produced, metallic egg beater shaped hairs (M. Mail & S. Schimmel, unpublished).

Materials for replication

All negative molds were produced out of agar gel. It was prepared by dissolving 3.6 g agar per 100ml in boiling water and letting it stir for 15 minutes.

Several low viscosity, 2 component silicones with different Shore hardnesses have been tested for the fillings:

- Elastosil RT 601 (viscosity: 3500 mPa s; hardness Shore A: 45)
- Elastosil RT 604 (viscosity: 800 mPa s; hardness Shore A: 25)
- Elastosil RT 607 (viscosity: 12000 mPa s; hardness Shore A: 55)

(All by Wacker Chemie AG, München, Germany)

Elastosil RT 607 was also used mixed with 1 percent carbon powder (Evonik Degussa GmbH, Germany) to increase hair stability.

Methods

Negative molding: The technical surface was glued to the base of a plastic box with a two component epoxy resin (Pattex Powerkleber Kraft Mix Extrem Schnell, Henkel AG & Co. KGaA, Düsseldorf, Deutschland). Then the agar gel was applied at 90 °C.

The *Salvina* leaves were glued to the bottom of a plastic box with super glue (UHU Sekundenkleber, UHU GmbH, Bühl, Germany). To provide total wetting with the agar gel the leaves were briefly coated with 70% percent ethanol solution just before molding. To prevent heat damage to the leaves the agar gel was cooled down to 45 °C under constant stirring and then poured onto the leaves until they were fully covered.

For both samples the agar gel was cooled to 26 - 29 °C before the templates were demolded by pulling them straight upwards out of the negative material. To remove water that would condense on or flow into the form from the surrounding agar the molds were stored in a vacuum (200 mbar) for 30 minutes prior to filling.

Production of positive replicas: The previously generated negative molds were filled with liquid silicone and immediately placed in a vacuum chamber. Pressure was slowly lowered to 50 mbar and kept there for 5 minutes to remove potential air bubbles between the mold and the filling material. Afterwards the pressure chamber was quickly vented and the specimen were placed in a heating cabinet at 35°C for 24 hours to cure. The plastic boxes were provided with some water and covered with a lid to prevent water loss of the agar gel, which would lead to shrinkage.

After hardening of the silicone the negative molds were dissolved in boiling water and dipped in Ethanol for faster drying afterwards.

The replicated samples were visually inspected and measured in a digital optical microscope (VHX-1000, Keyence, Japan).

6.3.2 Results and discussion

During replication several points proved to be critical for successful replication. The concentration of the agar gel had to be high enough to form a stable negative. A lower concentration also secreted more water into the mold after the template was removed. Too high concentrations resulted in a brittle consistency of the gel, which cause the agar to get pulled out of the mold inside the egg beater shapes. 3,6 g/100ml proved to be the optimal concentration for the samples tested. Small modifications might be necessary to adapt to different sizes and aspect ratios.

Another crucial parameter was the temperature during removal of the template. Too high temperatures would leave the gel to liquid and either the form would get filled up or at least the replication quality would suffer. Too low temperatures would again lead to a rather brittle consistency of the gel, preventing the arms of the egg beater shapes to cut through the material and resulting in gel getting stuck inside the egg beater hairs. Depending on the size of the template structures temperatures between 26°C and 29°C were optimal.

Further more capillary forces inside the negative mold would tend to fill the negative with water from the water content of the agar gel or condensed air humidity. This water would then prevent the silicone to fill the negative and result in poor replication results. To prevent this from happening the negatives were stored in a 200 mbar vacuum for 30 to 45 minutes prior to filling.

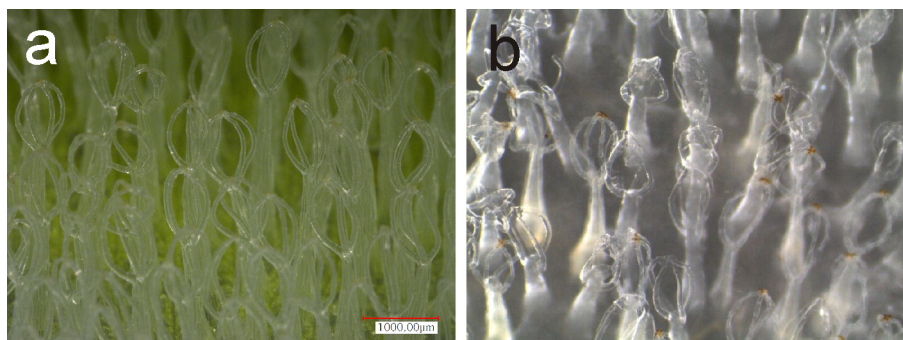


Figure 6.6: Comparison of hairs of *S. molesta*; a) original, b) replica (Elastosil RT 601, submerged)

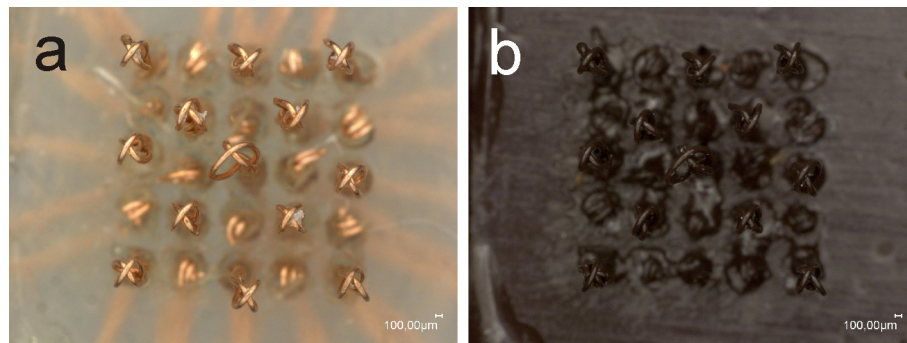


Figure 6.7: Comparison of an array of technical egg beater shaped hairs; a) original, b) replica (Elastosil RT 607 with 1% carbon)

Table 6.2: Quality of replication. Comparison of hair thickness and egg beater width of the template and the replicas (n=20)

		template	replica
hair thickness	μm	101.2 ± 4.2	102.8 ± 6.2
egg beater width	μm	629.1 ± 87.8	619.4 ± 86.9

The described replication technique was able to replicate *Salvinia* leaves as well as technical egg beater shaped hairs. In figure 6.6b even the cellular structure of the trichomes is visible in the replica. However, all three of the negative materials without carbon addition proved to be too elastic. The hairs would collapse under their own weight or stick together in groups unless they were stored under water. That is why the image in figure 6.6b could only be made under water. By adding 1% carbon powder to the hardest of the three silicones a kind of composite material was achieved that had enough stability to support the hair structures while being liquid enough to flow into the negative mold.

Replicas of the technical egg beater shaped hairs (Fig. 6.7b) were used to measure the quality of the replication process, because one template could be used for several replicas and measured afterwards, while the *Salvinia* leaves get damaged during the replication process.

Hair thickness and width of the egg beater shape was measured on the template as well as the replicas (n=20) (Table 6.2). As the results of the hair thickness show the replication technique displays a precision in the μm -scale. The value of the replicas lie within the standard deviation of the measurement. The standard deviation of the replicas is a little higher than the one of the template, which is to be expected due to little imperfections of the replication process. The values for the width of the egg beater shapes are also equivalent between the template and the replicas. This proves that the replication technique is capable of precisely reproducing closed loop structure with an accuracy in the μm -scale. With material costs of below 0.5 cent per cm^2 for the agar (75 EUR/kg; 100ml of 3.6% agar solution can replicate about 80 cm^2) and approximately 1 cent per cm^2 for the silicone (1g per cm^2 of 2mm height and 10 EUR/kg) this proves to be a promising low-cost method for the mass production of air retaining surfaces with closed-loop structures. The templates for the replication could be generated by one of the rapid prototyping techniques mentioned above.







6.4 Conclusion

To summarize the results of the technical surface it was proven that air retention could be achieved by different technical surfaces. The findings on the influence of hair density and height could be verified with flock material. It was also shown that the *Salvinia*[®]-effect can not only stabilize the air layer under pressure fluctuations but also improves the air layer persistence under static conditions. Furthermore a replication technique was developed that can be used for the cost efficient production of optimized air retaining surfaces in the future.

7 Design of an optimized technical surface

The investigations on the biological model organisms indicate that different species and thereby structure characteristics perform best in different stress tests (Table 7.1). While one surface structure is advantageous in one condition it can be unfavorable in others. So an optimal design for all conditions does not exist in nature. But the different tests performed show different advantages of the hair shapes that can be segregated and then united into a single new design incorporating these advantages.

Table 7.1: Overview of the performance of *Salvinia* hair structures and leaf shapes in different stress tests; - = bad, • = neutral, + = good

	 <i>S.</i> <i>oblongifolia</i>	 <i>S.</i> <i>cucullata</i>	 <i>S.</i> <i>minima</i>	 <i>S.</i> <i>molesta</i>	 hood shape	 oval shape
Long term stability	+	•	•	•	•	•
Pressure stability	-	•	•	+	+	•

The persistence tests indicate that diffusion is the main cause of air loss under static conditions. As the air volume loss by diffusion is proportional to the surface area of the air water interface a thick air layer would take longer to deplete, which is also obvious by the comparison of *S. molesta* to *S. cucullata* and *S. minima*. *S. oblongifolia* performs best under static conditions. Due to its dome shaped emergences this species held the air layer for the longest period of time and depleted its air layer only when the leaf started to decay.

Under changing pressure conditions the experiments also indicate advantages of thick air layers. While *S. oblongifolia* exhibits the longest air layer persistence in static conditions, its resistance to increasing hydrostatic pressure is worst of the examined species. *S. cucullata* on the other hand retains an air layer even at high pressures, because the air can form a bubble inside its hood shaped leaves. This however contradicts the design of the *Salvinia*[®]-effect, where every hair tip is hydrophilic and pinned to the air water interface. So both cannot be achieved completely at the same time.

A further advantage of the egg beater hairs of *S. molesta* gets apparent on the restoration of the air layers upon reducing the hydrostatic pressure. In the progress of air compression in between the hair an air bubble gets trapped inside the egg beater shape. Observations in the pressure cell as well as in dipping experiments performed at our partners at the KIT display a jump of the air water interface to the hair tip as soon as it reaches the air bubble from below. The small contact areas with the trichome branches and the extreme curvature the air water interface would have, if it was located between the tip of the emergences and the hair tip, result in an energetically unstable state. This causes the

water to snap to the tip of the hair when it reaches the air bubble inside the egg beater shape.

Flock experiments also proved that high hair densities increase the air layer persistence. However, with the application of drag reduction in mind this leads once again to a conflict. While the air layer stability increases with high densities so does the drag because of the higher contact area of water and solid.

Taking all this into account one ideal surface for the application in drag reducing ship coatings does not exist. Because of the counteracting effect of certain surface characteristics, trade offs have to be made between high stability and large drag reduction as well as to stability against high and low pressures (air bubbles vs. *Salvinia*[®]-effect).

A tradeoff design combining many beneficial aspects of the biological model organisms could look like displayed in Fig. 7.1. It is a hexagonal segment consisting of hairs with the dome shaped emergences of *S. oblongifolia* as well as the egg beater shapes of *S. molesta*. The segment is indented in its center to allow a air bubble to form in order to increase the stability against high pressures. Hydrophilic tips (displayed in red) of the *Salvinia*[®]-effect are only incorporated in the outer regions. As low pressures are not as much a problem in the envisioned applications as high pressures and air extraction by flow, this distribution of hydrophilic pins would allow the existence of a slight air bubble in the center while the *Salvinia*[®]-effect prevents the loss of air bubble at the edges, where they would be much more likely due to flow or a vertical orientation of the surface. The density of the structures should be in a range of about 15 to 20 per square millimeter (close to *S. cucullata* and *S. oblongifolia*) to have a more uniform behavior in pressure conditions compared to the local cave-ins observed on *S. molesta* and *S. minima*. The height should be at least 2 mm to provide a large volume of air, which proved to be beneficial in both persistence and pressure tests. Larger areas could be coated by stitching several of these hexagonal segments together. This would also prevent a loss of air on large vertical surfaces. The segmentation would prevent a continuous air layer in which the hydrostatic pressure would generate in a large pressure difference across the surface and result in pushing the air to the top.

A prototype of such a design could be produced by 3D laser lithography and reproduced for large scale application by the replication technique introduced in chapter 6. Different methods of hydrophobation would be possible; e.g. by galvanic copper structuring with subsequent Teflon coating or by a coating with self organizing nano particles.

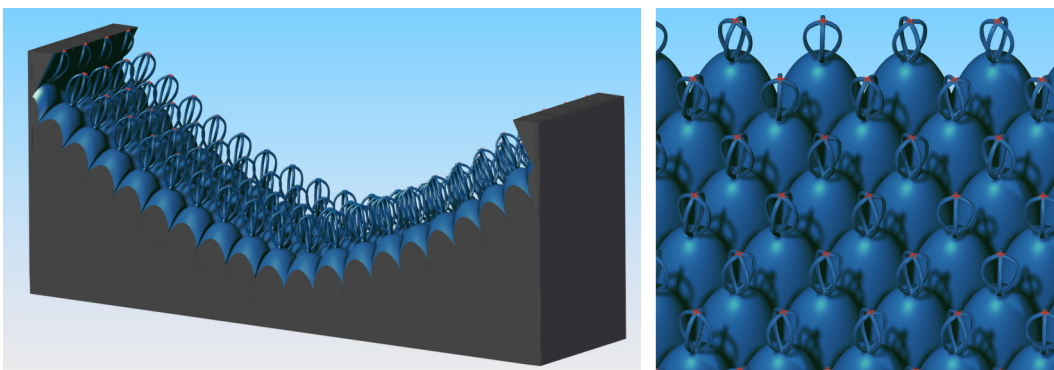


Figure 7.1: Design of a new technical air retaining surface a) side view of a segment, b) detail of the hair structures

Additionally other means for the stabilization and regeneration of such an air layer might be advisable to establish permanent air retention. One might be the injection of additional gas into the structure/air layer in order to refill it. One might also use a gas with a low solubility in water, thereby slowing down or inverting the air loss by diffusion. Further possibilities include gas delivery by electrophoresis of water, generated by thin wires attached just above the surface as electrodes or by the micro bubble technology.

Even if occasionally some air might be lost, one or several these measures would guarantee a permanent air layer on the surface. The minimal energy consumption for the regeneration of the air layer would be rather small compared to the huge potential a permanent air layer would have for the reduction of fuel consumption.

Summary

Mayser, Matthias J. (2013). *Air layers under water on the fern *Salvinia* – Stability and biomimetic applications*. Doctoral thesis, Mathematisch-Naturwissenschaftliche Fakultät, Rheinische Friedrich-Wilhelms-Universität Bonn.

Many plants and animals feature superhydrophobic surfaces capable of retaining a layer of air when submerged under water. The most persistent air layers can last for weeks and even month and are maintained by hairy surfaces structures. Such under water air retaining surfaces might be of high interest for future biomimetic applications e.g. drag reducing ship coatings. This study examines the air layer stability of four *Salvinia* species with different hair shapes under static and pressure conditions as well as the technical transfer of such air layers into technical application.

The air volumes held on *Salvinia*'s upper leaf surfaces is precisely measured. Therefor a new measurement setup based on strain gages is established which is capable of detecting air volumes under water with high resolution and a large detection range. The air volumes on the four different *Salvinia* species vary between 0.15 and 1 l/m² depending on the size of the corresponding hairs, their spacing and their volume.

The novel measurement system allows for the first time to monitor the volume of air layers and its decrease over time. With this method the air layer persistence of the different *Salvinia* species is described. Three species display a continuous air loss over time (excluding the influence of photosynthesis) caused by diffusion due to the pressure difference between the air in the gas film and the air above the surface. *S. oblongifolia* displays a completely different progress of air loss. It loses air in a two step process. Due to its dome shaped emergences the air water interface experiences a higher degree of support when it reaches the level of the emergences, achieves a higher curvature and can thereby counteract diffusion. The remaining air leaves the leaf only when it starts to decay.

The air layer stability under pressure fluctuations is analyzed. While three of the four species (all except *S. oblongifolia*) are capable of maintaining air on the surface under the pressures experienced on ship hulls (2.5 bar) the degree of air coverage on the surface and the restoration capabilities of the air layer after lowering the pressure to ambient conditions vary largely between the species. Because of its hood shaped leaves *S. cucullata* displays the best performance under pressure fluctuations. An air bubble is formed inside the leaf. Its volume gets pressed in between the hairs as pressure increases, but up to 6 bar a large portion of the surface remains covered with air. Accordingly the air layer restores almost completely after the pressure is released.

Different technical under water air retaining surfaces are investigated. Flock surfaces confirmed the influence of hair length, thickness and density on air layer persistence. Measurements with technical *Salvinia*[®]-effect surfaces also indicate that its hydrophilic pins not only prevent air bubble extraction from gas film but might also increase air layer

persistence in static conditions. The reasons are not fully understood though. Additionally a new low cost replication technique is presented which allows of reproducing closed loop structures like the sophisticated egg beater hairs and could hence be utilized for the production of large technical under water air retaining surfaces.

New insights in the stability of air layers are generated, design schemes deduced for new technical air retaining surfaces and a new production technique provided for such surfaces. Applied on ship hulls, micro fluidics or in the fluid transport systems these findings could have a high economic and ecologic value by leading to a substantial reduction in energy consumption.

Zusammenfassung

Mayser, Matthias J. (2013). *Air layers under water on the fern *Salvinia* – Stability and biomimetic applications*. Doctoral thesis, Mathematisch-Naturwissenschaftliche Fakultät, Rheinische Friedrich-Wilhelms-Universität Bonn.

Viele Pflanzen und Tiere besitzen superhydrophobe Oberflächen, die in der Lage sind, beim Untertauchen eine Luftschicht zu halten. Die langlebigsten dieser Luftschichten halten einige Wochen und sogar Monate und werden durch haarige Oberflächenstrukturen gehalten. Solche unter Wasser Luft haltenden Oberflächen könnten von enormer Bedeutung für bionische Anwendungen wie z.B. reibungsreduzierende Schiffsbeschichtungen sein. In dieser Arbeit wurde die Stabilität der Luftschichten von vier *Salvinia* Arten mit unterschiedlichen Haarstrukturen unter statischen und druckdynamischen Bedingungen sowie die Möglichkeit zur Übertragung der Luftschichten in die technische Anwendung untersucht.

Zunächst wurden die Luftvolumina, die auf den Blattoberseiten der *Salvinia* Blätter gehalten werden, präzise bestimmt. Dafür wurde eine neue auf Dehnungsmessstreifen basierende Messmethode entworfen, die in der Lage ist Luftvolumen unter Wasser mit hoher Präzision und einem großen Messbereich zu messen. Die gemessenen Luftmengen für die vier verschiedenen *Salvinia* Arten lagen im Bereich zwischen 0,15 und 1 l/m² abhängig von der Größe, dem Abstand und dem Volumen der für die Lufthaltung verantwortlichen Haare.

Diese neue Messmethode ermöglicht zusätzlich, die Veränderung der Luftmengen unter Wasser in Echtzeit zu verfolgen und ihre Veränderungen zu protokollieren. Dadurch konnte die Dauer der Lufthaltung und der Verlauf der Luftabnahme für die *Salvinia* Arten bestimmt werden. Bei allen Arten konnte (bei unterbundener Photosynthese) ein kontinuierlicher Luftverlust festgestellt werden, der in Relation zur Größe der Blattoberfläche steht und daher auf die Diffusion durch den Druckunterschied zwischen der Luft in der Luftschicht und dem Oberflächendruck gestellt werden konnte. Eine Besonderheit ergab sich bei *S. oblongifolia*, die im Gegensatz zu den anderen Arten einen zweistufigen Luftverlust aufwies. Aufgrund der kuppelförmigen Sockel der *S. oblongifolia* Haare wurde die Luft-Wasser-Grenzschicht beim Erreichen dieser stabilisiert. Dadurch ergab sich eine höhere Krümmung der Grenzschicht, die der Diffusion entgegenwirkte. Die restliche Luft ging in den Versuchen erst verloren, als sich ein Faulungsprozess der Blätter einstellte.

Bei den Untersuchungen zur Stabilität unter Druckbedingungen konnten drei der vier untersuchten Arten Luft bis zu den Drücken halten, die an einem Schiffsrumpf auftreten (2,5 bar). Allerdings ergaben sich große Unterschiede im Grad der Luftbedeckung und bezüglich der Regeneration der Luftschicht nach Druckablass. *S. cucullata* zeigte dabei durch ihre Blattform eine besondere Anpassung. Die tütenförmigen Blätter sind in der Lage eine Luftblase einzuschließen, die durch ihr zusätzliches Volumen eine stärkere Komprimierung der Luftschicht ermöglicht, bevor es zu einer Benetzung der Oberfläche

kommt. Selbst bei 6 bar Überdruck waren noch Teile der Oberfläche luftbedeckt. Dadurch ergab sich auch eine nahezu vollständige Wiederausbildung der Luftschicht nach Druckablass.

Bezüglich der technischen Umsetzung solcher Luftschichten wurden verschiedene künstliche Oberflächen untersucht. Mit Hilfe von unterschiedlichen Flockoberflächen konnte der Einfluss von Haarlänge, -dicke und -dichte auf die Stabilität der Luftschicht belegt werden. Des Weiteren wurden mit technischen Oberflächen Hinweise entdeckt, dass der *Salvinia*[®]-Effekt nicht nur den Verlust von Luftblasen bei Turbulenzen verhindert sondern auch unter statischen Bedingungen den Luftverlust verlangsamt. Die Gründe hierfür sind allerdings noch nicht vollständig aufgeklärt. Außerdem wurde eine neue, kostengünstige Replikationsmethode entwickelt, die es ermöglicht die geschlossenen, ringförmigen Strukturen der Schneebesenhaare abzubilden. Diese Methode könnte für die Produktion von technischen, unter Wasser Luft haltenden Oberflächen im größeren Maßstab verwendet werden.

Es konnten neue Einblicke in die Zusammenhänge der Lufthaltung erreicht, neue Oberflächendesigns für Luft haltende Oberflächen abgeleitet und eine passende Herstellungsmethode entwickelt werden. Eine mögliche Anwendung dieser Erkenntnisse in Schifffahrt, Mikrofluidik oder anderen Wassertransportsystemen würde große ökonomische und ökologische Nutzen mit sich bringen und einen bedeutenden Beitrag zur Verringerung des Energieverbrauchs leisten.

List of Figures

1.1	The contact angle established between liquid and solid	1
1.2	Hydrophilic and hydrophobic wetting	2
1.3	Cassie-Baxter-state and Wenzel-state	2
1.4	Air layer on <i>S. oblongifolia</i>	4
1.5	Principle of drag reduction by air layers	5
1.6	Air layer on <i>Salvinia molesta</i>	6
1.7	Surface structures of <i>N. glauca</i>	7
1.8	<i>Salvinia cucullata</i>	9
1.9	<i>Salvinia oblongifolia</i>	9
1.10	<i>Salvinia minima</i>	10
1.11	<i>Salvinia molesta</i>	10
1.12	Salvinia [®] -effect	11
3.1	SEM images of wafer replicas	15
3.2	SEM images of the examined <i>Salvinia</i> surface	16
3.3	Buoyancy measurement setup	17
3.4	Circuit diagram	17
3.5	Measurement calibration graph	18
3.6	Air volume measured on structured wafer replicas	18
3.7	Air volume per surface area on four different <i>Salvinia</i>	20
3.8	Comparison of theoretical and measured air volume on <i>Salvinia</i>	21
4.1	Temperature sensitivity of the measurement setup	23
4.2	temperature stabilized by heating elements	24
4.3	Aerenchyma of <i>S. oblongifolia</i>	25
4.4	False air loss measurement on <i>S. oblongifolia</i>	25
4.5	Comparison of the air decrease on <i>Salvinia</i>	26
4.6	Hair structures on <i>Salvinia</i>	27
4.7	Changes of air volume over time on <i>Salvinia</i>	28
4.8	Air loss rates per surface area on <i>Salvinia</i>	29
4.9	Relative changes of air volume over time on <i>Salvinia</i>	30
5.1	Scheme of the pressure cell	32
5.2	Setup of the pressure cell	33
5.3	Air layer on <i>S. minima</i> during a pressure cycle	34
5.4	Air layer on <i>S. molesta</i> during a pressure cycle	35
5.5	Air layer on <i>S. oblongifolia</i> during a pressure cycle	35
5.6	Air layer on <i>S. cucullata</i> during a pressure cycle	36
5.7	Pressure of first air layer collapse on <i>Salvinia</i>	37
5.8	Pressure with no air between <i>Salvinia</i> trichomes	38
5.9	Percentage of air layer regeneration	39

6.1	Sample of flock surfaces	42
6.2	Setup for air layer persistence testing on flock	43
6.3	Air layer Persistence on flock surfaces	44
6.4	Comparison of changes in air volume on small technical surfaces	45
6.5	Comparison of changes in air volume on big technical surfaces	46
6.6	Original and replica of <i>S. molesta</i>	48
6.7	Original and replica of technical egg beater hairs	49
7.1	Design of a new technical air retaining surface	52

List of Tables

3.1	Structure characteristics of 4 selected <i>Salvinia</i> species ($m \pm s.d.$, $n=10$) . . .	19
4.1	Initial air loss of 4 selected <i>Salvinia</i> species ($m \pm s.d.$)	28
6.1	Structure parameters of the flock samples used	42
6.2	Quality of replication. Comparison of hair thickness and egg beater width of the template and the replicas ($n=20$)	49
7.1	Overview of the performance of <i>Salvinia</i>	51

Bibliography

- Atkins, Peter W.; de Paula, J. (2006). *Physikalische Chemie*. Wiley-VCH Verlag, Berlin, 4. vollständig überarbeitete edition. ISBN 3527315462.
- Balasubramanian, A., Miller, A., and Rediniotis, O. (2004). Microstructured hydrophobic skin for hydrodynamic drag reduction. *AIAA Journal*, 42(2):411–414.
- Balmert, A., Bohn, H. F., Ditsche-Kuru, P., and Barthlott, W. (2011). Dry under water: Comparative morphology and functional aspects of air-retaining insect surfaces. *Journal of Morphology*, 272(4):442–451.
- Barthlott, W. (1990). Scanning electron microscopy of the epidermal surface in plants. In Claugher, D., editor, *Application of the scanning EM in taxonomy and functional morphology*, Systematics Association's Special Volume, pages 69–94. Clarendon Press, Oxford.
- Barthlott, W. and Koch, K., editors (2011). *Biomimetic materials (special issue)*, Beilstein Journal of Nanotechnology. Beilstein-Institute, Frankfurt a.M.
- Barthlott, W. and Neinhuis, C. (1997). Purity of the sacred lotus, or escape from contamination in biological surfaces. *Planta*, 202:1–8.
- Barthlott, W., Riede, K., and Wolter, M. (1994). Mimicry and ultrastructural analogy between the semi-aquatic grasshopper *Paulinia acuminata* (Orthoptera: Pauliniidae) and its foodplant, the water-fern *Salvinia auriculata* (Filicatae: Salviniaceae). *Amazoniana*, 13:47–58.
- Barthlott, W., Schimmel, T., Wiersch, S., Koch, K., Brede, M., Barczewski, M., Walheim, S., Weis, A., Kaltenmaier, A., Leder, A., and Bohn, H. F. (2010). The *Salvinia* Paradox: Superhydrophobic Surfaces with Hydrophilic Pins for Air Retention Under Water. *Advanced Materials*, 22(21):2325–2328.
- Barthlott, W., Wiersch, S., Colic, Z., and Koch, K. (2009). Classification of trichome types within species of the water fern *Salvinia*, and ontogeny of the egg-beater trichomes. *Botany*, 87(9):830–836.
- Barthlott, W. and Wollenweber, E. (1981). Zur Feinstruktur, Chemie und taxonomischen Signifikanz epicuticularer Wachse und ähnlicher Sekrete. *Tropische und subtropische Pflanzenwelt*, 32:7–67.
- Beneski, J. T. and Stinson, D. W. (1987). *Sorex palustris*. *Mammalian Species*, 296:1–6.
- Bhushan, B. (2004). *Springer handbook of nanotechnology*. Springer Verlag, Berlin, Heidelberg, New York, 1 edition. ISBN: 3540012184.

- Bhushan, B., Nosonovsky, M., and Chae Jung, Y. (2007). Towards optimization of patterned superhydrophobic surfaces. *Journal of The Royal Society Interface*, 4(15):643–648.
- Breuer, H. J. (2010). Antifouling fibre coatings for marine constructions. Patent Nr. US 2010/0227111 A1.
- Bush, J. W. and Hu, D. L. (2006). Walking on water: Biocomotion at the Interface. *Annual Review of Fluid Mechanics*, 38(1):339–369.
- Calder, W. (1969). Temperature relations and underwater endurance of the smallest homeothermic diver, the water shrew. *Comparative Biochemistry and Physiology*, 30(6):1075–1082.
- Callies, M. and Quéré, D. (2005). On water repellency. *Soft Matter*, 1(1):55–61.
- Cassie, A. and Baxter, S. (1944). Wettability of porous surfaces. *Transactions of the Faraday Society*, 40:546–551.
- Chen, W., Fadeev, A. Y., Hsieh, M. C., Öner, D., Youngblood, J., and McCarthy, T. J. (1999). Ultrahydrophobic and Ultralyophobic Surfaces: Some Comments and Examples. *Langmuir*, 15:3395–3399.
- Cheng, Y. T., Rodak, D. E., Wong, C. A., and Hayden, C. A. (2006). Effects of micro- and nano-structures on the self-cleaning behaviour of lotus leaves. *Nanotechnology*, 17(5):1359–1362.
- Choi, C.-H. and Kim, C.-J. (2006). Large slip of aqueous liquid flow over a nanoengineered superhydrophobic surface. *Physical Review Letters*, 96:66001.
- Colmer, T. D. and Pedersen, O. (2008). Underwater photosynthesis and respiration in leaves of submerged wetland plants: gas films improve CO₂ and O₂ exchange. *New Phytologist*, 177(4):918–926.
- Corbett, J. J. and Koehler, H. W. (2003). Updated emissions from ocean shipping. *Journal of Geophysical Research*, 108(D20):4650–4664.
- Crisp, D. J. (1950). The stability of structures at a fluid interface. *Transactions of the Faraday Society*, 46:228–235.
- De Gennes, P. (1985). Wetting: statics and dynamics. *Reviews of Modern Physics*, 57(3 (Part I)):827–863.
- De Gennes, P.-G., Brochard-Wyart, F., and Quéré, D. (2004). *Capillarity and wetting phenomena. Drops, bubbles, pearls, waves*. Springer, New York, Berlin, Heidelberg.
- De la Sota, E. R. (1977). Índice sistemático y bibliográfico de los taxa vivientes del género "Salvinia" Adanson (Salviniaceae - Pteridophyta). In *Obra del Centenario del Museo de La Plata*, volume 3, pages 229–235. La Plata.
- Ditsche-Kuru, P., Mayser, M. J., Schneider, E. S., Bohn, H. F., Koch, K., Melskotte, J.-E., Brede, M., Leder, A., Barczewski, M., Weis, A., Kaltenmaier, A., Walheim, S., Schimmel, T., and Barthlott, W. (2011a). Eine Lufthülle für Schiffe - Können Schwimmpflanzen und Rückenschwimmer helfen Sprit zu sparen? In Kesel, A. B. and Zehren, D., editors, *Bionik: Patente aus der Natur - 5. Bremer Bionik Kongress*, pages 159–165, Bremen. Kesel, A. B. & Zehren, D.

- Ditsche-Kuru, P., Schneider, E. S., Melskotte, J.-E., Brede, M., Leder, A., and Barthlott, W. (2011b). Superhydrophobic surfaces of the water bug *Notonecta glauca*: a model for friction reduction and air retention. *Beilstein Journal of Nanotechnology*, 2:137–144.
- Ege, R. (1915). On the respiratory function of the air stores carried by some aquatic insects (Corixidae, Dytiscidae and Notonecta). *Zeitschrift für Allgemeine Physiologie*, 17:18–124.
- Eriksen, C., Resh, V., Balling, S., and Lamberti, G. (1995). *An Introduction to the Aquatic Insects of North America*, chapter Aquatic insect respiration, pages 27–37. Kendall Hunt Publishing Company, Debique, Iowa, 3 edition. ISBN: 0787232416.
- Eyring, V., Isaksen, I. S. A., Berntsen, T., Collins, W. J., Corbett, J. J., Endresen, O., Grainger, R. G., Moldanova, J., Schlager, H., and Stevenson, D. S. (2010). Transport impacts on atmosphere and climate: Shipping. *Atmospheric Environment*, 44(37):4735–4771.
- Flynn, M. R. and Bush, J. W. M. (2008). Underwater breathing: the mechanics of plastron respiration. *Journal of Fluid Mechanics*, 608:275–296.
- Forsberg, P., Nikolajeff, F., and Karlsson, M. (2011). Cassie-Wenzel and Wenzel-Cassie transitions on immersed superhydrophobic surfaces under hydrostatic pressure. *Soft Matter*, 7(1):104–109.
- Fukagata, K., Kasagi, N., and Koumoutsakos, P. (2006). A theoretical prediction of friction drag reduction in turbulent flow by superhydrophobic surfaces. *Physics of Fluids*, 18:1–8.
- Fukuda, K., Tokunaga, J., Nobunaga, T., Nakatani, T., Iwasaki, T., and Kunitake, Y. (2000). Frictional drag reduction with air lubricant over a super-water-repellent surface. *Journal of Marine Science and Technology*, 5(3):123–130.
- Furmidge, C. (1962). Studies at phase interfaces: I. The sliding of liquid drops on solid surfaces and a theory for spray retention. *Journal of colloid science*, 17:309–324.
- Gao, L. and McCarthy, T. J. (2007). How Wenzel and Cassie Were Wrong. *Langmuir*, 23(7):3762–3765.
- Gao, L. and McCarthy, T. J. (2009). Wetting 101. *Langmuir*, 25(24):14105–14115.
- Germanischer-Lloyd (2011). Bauvorschriften & Richtlinien. Technical report, Germanische rLloyd, Hamburg.
- Greenwood, Norman N.; Earnshaw, A. (1997). *Chemistry of the Elements*. Butterworth-Heinemann, Oxford, 2. edition. ISBN 0750633654.
- Hebets, E. and Chapman, F. (2000). Surviving the flood: plastron respiration in the non-tracheate arthropod *Phrynus marginemaculatus* (Amblypygi: Arachnida). *Journal of Insect Physiology*, 46(1):13–19.
- Heckman, C. W. (1983). Comparative Morphology of Arthropod Exterior Surfaces with the Capability of Binding a Film of Air Underwater. *Internationale Revue der gesamten Hydrobiologie und Hydrographie*, 68(5):715–736.

- Herzog, R. (1934). Anatomische und experimentell-morphologische Untersuchungen über die Gattung *Salvinia*. *Planta*, 22(4):490–514.
- Hutchinson, G. E. (1981). Thoughts on aquatic insects. *Bioscience*, 31(7):495–500.
- International Energy Agency (2009). *Transport, Energy and Co2: Moving Toward Sustainability*. Organisation for Economic Co-Operation and Development (OECD). ISBN 9264073167.
- Jacono, C., Davern, T., and Center, T. (2001). The Adventive Status of *Salvinia minima* and *S. molesta* in the Southern United States and the Related Distribution of the Weevil *Cyrtobagous salviniae*. *Castanea*, 66(3):214–226.
- Julien, M. H., Center, T. D., and Tipping, P. W. (2002). *Biological Control of Invasive Plants in the Eastern United States*, chapter Floating Fern (SALVINIA), pages 17–32. USDA Forest Service Publication.
- Jung, Y. C. and Bhushan, B. (2006). Contact angle, adhesion and friction properties of micro- and nanopatterned polymers for superhydrophobicity. *Nanotechnology*, 17(19):4970–4980.
- Kaeding, P. (2009). Belastung des Schiffbodens nach GL. Technical report, ThyssenKrupp Marine Systems.
- Kaul, R. B. (1976). Anatomical observations on floating leaves. *Aquatic Botany*, 2:215–234.
- Köhler, D. (1991). Notes on the diving behaviour of the water shrew, *Neomys fodiens* (Mammalia, Soricidae). *Zoologischer Anzeiger*, 227:218–228.
- Kim, J. and Kim, C.-J. (2002). Nanostructured surfaces for dramatic reduction of flow resistance in droplet-based microfluidics. In *Proceedings of the Fifteenth IEEE International Conference on Micro Electro Mechanical Systems, 20-24 Jan. 2002, Las Vegas*, pages 479–482. Institute of Electrical and Electronics Engineers, Washington, D.C.
- Koch, K. and Barthlott, W. (2009). Superhydrophobic and superhydrophilic plant surfaces: an inspiration for biomimetic materials. *Philosophical Transactions of the Royal Society A: Mathematical, Physical and Engineering Sciences*, 367(1893):1487–1509.
- Koch, K., Bhushan, B., and Barthlott, W. (2008a). Diversity of structure, morphology and wetting of plant surfaces. *Soft Matter*, 4(10):1943–1963.
- Koch, K., Bohn, H. F., and Barthlott, W. (2009). Hierarchically Sculptured Plant Surfaces and Superhydrophobicity. *Langmuir*, 25(24):14116–14120.
- Koch, K. and Ensikat, H.-J. (2008). The hydrophobic coatings of plant surfaces: Epicuticular wax crystals and their morphologies, crystallinity and molecular self-assembly. *Micron*, 39(7):759–772.
- Koch, K., Schulte, A. J., Fischer, A., Gorb, S. N., and Barthlott, W. (2008b). A fast, precise and low-cost replication technique for nano- and high-aspect-ratio structures of biological and artificial surfaces. *Bioinspiration & Biomimetics*, 3(4):046002.

- Kodama, Y., Kakugawa, A., Takahashi, T., Nagaya, S., and Sugiyama, K. (2003). Microbubbles: Drag reduction mechanism and applicability to ships. In *24th Symposium on Naval Hydrodynamics, Fukuoka, Japan*, pages 1–20. The National Academies Press, Washington.
- Konrad, W., Apeltauer, C., Frauendiener, J., Barthlott, W., and Roth-Nebelsick, A. (2009). Applying Methods from Differential Geometry to Devise Stable and Persistent Air Layers Attached to Objects Immersed in Water. *Journal of Bionic Engineering*, 6(4):350–356.
- Lake, M. (2009). *Oberflächentechnik in der Kunststoffverarbeitung: Vorbehandeln, Beschichten, Funktionalisieren und Kennzeichnen von Kunststoffoberflächen*. Carl Hanser Verlag GmbH & CO. KG. ISBN: 3446418490.
- Lakes, R. (1993). Materials with structural hierarchy. *Nature*, 361(6412):511–515.
- Larsén, O. (1955). Spezifische Mechanorezeptoren bei *Aphelocheirus aestivalis* Fabr. nebst Bemerkungen über die Respiration dieser Wanze. *Lunds Universitets Arsskrift*, 66(11):3–59.
- Lee, C. and Kim, C.-J. (2011). Underwater Restoration and Retention of Gases on Superhydrophobic Surfaces for Drag Reduction. *Phys. Rev. Lett.*, 106:014502.
- Liu, G., Fu, L., Rode, A. V., and Craig, V. S. J. (2011). Water Droplet Motion Control on Superhydrophobic Surfaces: Exploiting the Wenzel-to-Cassie Transition. *Langmuir*, 27(6):2595–2600.
- Marmur, A. (2006a). Super-hydrophobicity fundamentals: implications to biofouling prevention. *Biofouling*, 22(2):107–115.
- Marmur, A. (2006b). Underwater superhydrophobicity: Theoretical Feasibility. *Langmuir*, 22:1400–1402.
- Martin, J. and Juniper, B. (1970). *The cuticles of plants*. Edward Arnold Ltd, London, Edinburgh. ISBN 7131-2245-5.
- McHale, G., Aqil, S., Shirtcliffe, N. J., Newton, M. I., and Erbil, H. Y. (2005). Analysis of droplet evaporation on a superhydrophobic surface. *Langmuir*, 21.
- McHale, G., Flynn, M. R., and Newton, M. I. (2011). Plastron induced drag reduction and increased slip on a superhydrophobic sphere. *Soft Matter*, 7(21):10100–10107.
- McHale, G., Newton, M. I., and Shirtcliffe, N. J. (2010). Immersed superhydrophobic surfaces: Gas exchange, slip and drag reduction properties. *Soft Matter*, 6(4):714–719.
- Melskotte, J.-E., Brede, M., Leder, A., Mayser, M., and Barthlott, W. (2012). Optical Determination of the Velocity Field Over the Air-Retaining Elytra of *Notonecta glauca*. *tm - Technisches Messen*, 79(6):297–303.
- Messner, B. and Adis, J. (1996). Über die Vielfalt der Plastronatmung - Vorschlag zur Neufassung des Begriffes "Plastron". In *Verhandlungen Westdeutscher Entomologentag, Düsseldorf*, pages 89–92.
- Neinhuis, C. and Barthlott, W. (1997). Characterization and distribution of water-repellent, self-cleaning plant surfaces. *Annals of Botany*, 79:667–677.

- Nishino, T., Meguro, M., Nakamae, K., Matsushita, M., and Ueda, Y. (1999). The lowest surface free energy based on -CF₃ alignment. *Langmuir*, 15:4321–4323.
- Öner, D. and McCarthy, T. J. (2000). Ultrahydrophobic surfaces. Effects of topography length scales on wettability. *Langmuir*, 16(20):7777–7782.
- Otten, A. and Herminghaus, S. (2004). How plants keep dry: A physicist’s point of view. *Langmuir*, 20:2405–2408.
- Paffett, J. A. H. (1972). Improvements in and relating to water-borne vessels. Patent Nr. UK 1 300 132.
- Parsons, M. C. (1971). Respiratory significance of the external morphology of adults and fifth instar nymphs of *Notonecta undulata* Say (Aquatic heteroptera; Notonectidae). *Journal of Morphology*, 133(2):125–138.
- Perez Goodwyn, P. (2009). *Functional surfaces in biology*, volume 1, chapter Anti-wetting surfaces in Heteroptera (Insecta): Hairy solutions to any problem, pages 55–76. Springer, Dordrecht, Netherlands. ISBN: 1402099940.
- Quéré, D., Lafuma, A., and Bico, J. (2003). Slippery and sticky microtextured solids. *Nanotechnology*, 14:1109–1112.
- Raven, J. A. (2008). Not drowning but photosynthesizing: probing plant plastrons. *New Phytologist*, 177(4):841–845.
- Roach, P., Shirtcliffe, N. J., and Newton, M. I. (2008). Progress in superhydrophobic surface development. *Soft Matter*, 4(2):224–240.
- Schneller, J. J. (1990). *Pteridophytes and gymnosperms*, volume 1 of *The families and genera of vascular plants*, chapter Salviniaceae, pages 256–258. Springer, Berlin.
- Solga, A., Cerman, Z., Striffler, B. F., Spaeth, M., and Barthlott, W. (2007). The dream of staying clean: Lotus and biomimetic surfaces. *Bioinspiration & Biomimetics*, 2(4):1–9.
- Suter, R., Stratton, G., and Miller, P. (2003). Water surface locomotion by spiders: distinct gaits in diverse families. *Journal of Arachnology*, 31:428–432.
- Suter, R., Stratton, G., and Miller, P. (2004). Taxonomic variation among spiders in the ability to repel water: surface adhesion and hair density. *Journal of Arachnology*, 32(1):11–21.
- Suter, R. and Wildman, H. (1999). Locomotion on the water surface: hydrodynamic constraints on rowing velocity require a gait change. *The Journal of Experimental Biology*, 202:2771–2785.
- Thorpe, W. and D.J., C. (1947). Studies on plastron respiration III. The orientation responses of *Aphelocheirus* (Hemiptera, Aphelocheiridae (Naucoridae)) in relation to plastron respiration; together with an account of specialized pressure receptors in aquatic insects. *Journal of Experimental Biology*, 24:310–328.
- Thorpe, W. H. and Crisp, D. (1947a). Studies on plastron respiration. I. The biology of *Aphelocheirus* (Hemiptera, Aphelocheiridae) (Naucoridae), and the mechanism of plastron retention. *Journal of Experimental Biology*, 24:227–269.

- Thorpe, W. H. and Crisp, D. (1947b). Studies on plastron respiration. II. The respiratory efficiency of the plastron in *Aphelocheirus*. *Journal of Experimental Biology*, 24:270–303.
- Verho, T., Korhonen, J. T., Sainiemi, L., Jokinen, V., Bower, C., Franze, K., Franssila, S., Andrew, P., Ikkala, O., and Ras, R. H. A. (2012). Reversible switching between superhydrophobic states on a hierarchically structured surface. *Proceedings of the National Academy of Sciences*, 109(26):10210–10213.
- Vogel, S. (2006). Living in a physical world VIII. Gravity and life in water. *Journal of Biosciences*, 31(3):309–322.
- Wagner, P., Fürstner, R., Barthlott, W., and Neinhuis, C. (2003). Quantitative assessment to the structural basis of water repellency in natural and technical surfaces. *Journal of Experimental Botany*, 54(385):1295–1303.
- Wenzel, R. (1936). Resistance of solid surfaces to wetting by water. *Industrial and Engineering Chemistry*, 28(8):988–994.
- Wigglesworth, V. B. (1984). *Insect physiology*, volume 22. Springer Verlag, Berlin, 8. edition. ISBN 0412264609.
- Yan, Y., Gao, N., and Barthlott, W. (2011). Mimicking natural superhydrophobic surfaces and grasping the wetting process: A review on recent progress in preparing superhydrophobic surfaces. *Advances in Colloid and Interface Science*, 169(2):80 – 105.
- Young, T. (1805). An essay on the cohesion of fluids. *Philosophical Transactions of the Royal Society of London*, 95:65–87.
- Yu, X., Wang, Z., and Zhang, X. (2006). Surface gradient material: From superhydrophobicity to superhydrophilicity. *Langmuir*, 22:4483–4486.

Publications

Publications

- M.J. Mayser, M. Reker, H.F. Bohn and W. Barthlott (2014). Measuring air volumes retained by submerged technical and biological superhydrophobic surfaces. *Beistein Journal of Nanotechnology*, accepted
- M.J. Mayser and W. Barthlott (2014). Layers of air in the water on the floating fern *Salvinia* are exposed to fluctuations in pressure. *Integrative and Comparative Biology*, accepted
- H.J. Ensikat, M.J. Mayser and W. Barthlott (2012). Superhydrophobic and Adhesive Properties of Surfaces: Testing the Quality by an Elaborated Scanning Electron Microscopy Method. *Langmuir*, 28(40):14338-14346
- J.-E. Melskotte, M. Brede, A. Leder, M.J. Mayser, W. Barthlott (2012). Optical Determination of the Velocity Field Over the Air-Retaining Elytra of *Notonecta glauca*. *Technisches Messen*, 79(6):297-302.
- P. Ditsche-Kuru*, M.J. Mayser*, E.S. Schneider, H.F. Bohn, K. Koch, J.-E. Melskotte, M. Brede, A. Leder, M. Barczewski, A. Weis, A. Kaltenmaier, S. Walheim, T. Schimmel and W. Barthlott (2011). Eine Lufthülle für Schiffe - Können Schwimmarfarn und Rückenschwimmer helfen Sprit zu sparen? In: *Bionik: Patente aus der Natur - 5. Bremer Bionik Kongress, Bremen*, Kesel, A. B. and Zehren, D., ISBN 978-3-00-033467-2, pp. 159-165. (*contributed equally)
- J.-E. Melskotte, M. Brede, W. Wriggers, M.J. Mayser, A. Leder, and W. Barthlott (2011). Luft haltende Oberflächen zur Reibungsreduktion - künstliche Oberflächen und ihre biologischen Vorbilder. In: *Lasermethoden in der Strömungsmesstechnik, 19. Fachtagung, 6. - 8. September 2011, Ilmenau, Karlsruhe, Dt. Ges. für Laser-Anemometrie*, Thess, A.; Resagk, C.; Ruck, B.; Leder, A. (Eds.), pp. 23.1-23.6, 2011, ISBN 978-3-9805613-7-2

Patents

- E.S. Schneider, M.J. Mayser, P. Ditsche-Kuru, W. Barthlott, S. Walheim and T. Schimmel (2011), Unbenetzbare Oberflächen, Patent-Nr.: DE 102011121796.0
- A. Klein, M.J. Mayser, H. Herzog, W. Barthlott and H. Bleckmann (2012), Replikationsmethode für ringförmige Strukturen, Patent-Nr.: DE 102012212431

Conference presentations

- M.J. Mayser, W. Barthlott and T. Gilet (**2014**). The hairy, superhydrophobic surfaces on the water fern *Salvinia* - underwater air retention and raindrop impacts. *SICB Annual Meeting 2014*, Austin, Texas
- M.J. Mayser and W. Barthlott (**2011**). Lufthaltung untergetauchter, biologischer Oberflächen und ihr biomimetisches Potential. *DGL Jahrestagung 2011*, Freising-Weihenstephan
- P. Ditsche-Kuru*, M.J. Mayser*, E.S. Schneider, H.F. Bohn, K. Koch, J.-E. Mel-skotte, M. Brede, A. Leder, M. Barczewski, A. Weis, A. Kaltenmaier, S. Walheim, T. Schimmel and W. Barthlott (**2010**). Eine Lufthülle für Schiffe - Können Schwim-farn und Rückenschwimmer helfen Sprit zu sparen?, *Patente aus der Natur - 5. Bremer Bionik Kongress*, Bremen (*contributed equally)
- M. Mayser, P. Ditsche-Kuru, M. Brede, A. Leder, T. Schimmel and W. Barthlott (**2010**): Slipping through the water: Biological under water air retaining surfaces as a biomimetic approach to drag reduction. *Materials Science and Engineering 2010*, Darmstadt
- M. Mayser, H.F. Bohn, M. Brede, A. Leder and W. Barthlott (**2009**): Pflanzliche, unter Wasser Luft haltende Oberflächen und ihr biomimetisches Potential, *DGL Jahrestagung 2009*, Oldenburg

Posters

- M.J. Mayser and W. Barthlott (**2013**). Air layers under water on the water fern *Salvinia* exposed to pressure fluctuations. *Droplets 2013*, Marseilles